

SILVER(I)-CATALYZED OXIDATION OF CYCLIC SECONDARY AMINES  
WITH PEROXODISULFATE  
AND  
CONFORMATIONAL ANALYSIS OF THE PRODUCTS

by  
Keiichiro OGAWA

A Thesis  
Submitted to The University of Tokyo for the Degree of  
Doctor of Science  
July, 1983

## ACKNOWLEDGMENT

I wish to thank Professor Yujiro Nomura for his close guidance and constant encouragement throughout this work, Professor Hiroshi Suzuki and Professor Yoshito Takeuchi for their inspiring advices, and Dr. Shuji Tomoda for his valuable suggestions. I also thank Professor Kiyoshi Mutai, Professor Keiji Kobayashi, and Dr. Masato Ito for helpful discussions.

I am deeply grateful to Professor Michinori Ōki for the permission to use DNMR3 and LSQM2 programs and Professor Eiji Ōsawa of Hokkaido University for offering the program for molecular mechanics calculation MMI and for his valuable comments. I also thank Dr. Atsushi Tomonaga, Dr. Kenji Kasai, and Dr. Hiroshi Chuman of Kureha Chemical Ind. Co., Ltd for offering the program ZMMIP for generating coordinate data and the program MMI, and Dr. Akiko Itai of the University of Tokyo for her help in the use of MMI on the HITAC M-280H computer system of Computer Centre University of Tokyo. In addition I would like to thank Professor Naoki Inamoto for the permission to use spinning band distillation apparatus, Dr. Hiroshi Hirota for the measurements of the high resolution mass spectra, and Professor Shigeo Nishimura of Tokyo University of Agriculture and Technology for his help and advice in the catalytic hydrogenation. I am

especially grateful to Miss Toshiko Seki and Mrs. Kimiyo Saeki for performing elemental analyses.

## CONTENTS

Chapter 1. Silver(I)-catalyzed Oxidation of Cyclic Secondary Amines with Peroxodisulfate	
1.1 Introduction	1
1.2 Results and Discussion	2
1.3 Experimental	10
1.4 References	22
Chapter 2. Conformational Analysis of the Trimer of 2,3,4,5-Tetrahydro-4-methylpyridine	
2.1 Introduction	25
2.2 Results and Discussion	27
2.3 Experimental	40
2.4 References	42
Chapter 3. $^{13}\text{C}$ and $^1\text{H}$ NMR Study of 1-Pyrroline	
3.1 Introduction	43
3.2 Results and Discussion	44
3.3 Experimental	49
3.4 References	50
Chapter 4. Barriers to Rotation and Inversion in meso-1,1'-Bi(2-methylpiperidine)s	
4.1 Introduction	51
4.2 Synthesis of Materials	57
4.3 $^{13}\text{C}$ NMR Spectra of cis- and trans- 4-tert-Butyl-2-methylpiperidine	58

4.4 Variable Temperature $^{13}\text{C}$ NMR of	
meso-1,1'-Bi(2-methylpiperidine)s	61
4.5 Discussion	67
4.6 Experimental	92
4.7 Assignment of $^{13}\text{C}$ NMR Signals	
of meso-1,1'-Bi(2-methylpiperidine)s	100
4.8 Molecular Mechanics Calculation	103
4.9 References and Notes	105

#### Appendix 1.

Collected Papers for the Thesis

#### Appendix 2.

Collected Papers for Other Subjects

## LIST OF TABLES

Table 1.1	
Silver(I)-catalyzed Oxidation of Piperidines with Peroxodisulfate	3
Table 2.1	
Major Fragment Ions of the Trimer of 2,3,4,5- Tetrahydro-4-methylpyridine in High Resolution Mass Spectroscopy	28
Table 2.2	
Observed and Calculated $^{13}\text{C}$ Chemical Shifts for the Trimer of 2,3,4,5-Tetrahydro-4-methylpyridine	33
Table 2.3	
Molecular Mechanics Calculation of the Trimer of 2,3,4,5-Tetrahydro-4-methylpyridine	37
Table 3.1	
The Equilibrium Constant K of the Equilibrium between 1-Pyrroline and 1-Pyrroline Trimer	49
Table 4.1	
$^{13}\text{C}$ NMR Spectra of cis- and trans-	

4-tert-Butylpiperidine in $\text{CDCl}_3$	60
Table 4.2	
$^{13}\text{C}$ NMR Data for meso-1,1'-Bi(2-methylpiperidine)s	62
Table 4.3	
Activation Parameters for Conformational Process in meso-1,1'-Bi(cis-2-methylpiperidine)s	66
Table 4.4	
Molecular Mechanics Calculation of the Corresponding Hydrocarbons for the Bipiperidines	79
Table 4.5	
Comparison of the Observed Barriers of the Bipiperidines with the Calculated Rotational Barriers and the Calculated Steric Energies of the Trans Conformations Involved in the Inversion Paths in the Corresponding Hydrocarbons	89

## LIST OF FIGURES

### Figure 1.1

Tentative scheme for the silver(I)-catalyzed  
oxidation of cyclic secondary amines 9

### Figure 2.1

22.5 MHz  $^{13}\text{C}$  NMR of the trimer of 2,3,4,5-tetrahydro-  
4-methylpyridine in  $\text{CDCl}_3$  29

### Figure 2.2

Conformational interconversion in the trimer of  
2,3,4,5-tetrahydro-4-methylpyridine formed by the  
combination of one molecule of the monomer with  
R configuration and two molecules of the monomer  
with S configuration 32

### Figure 2.3

Conformational interconversion in the trimer of  
2,3,4,5-tetrahydro-4-methylpyridine formed by the  
combination of three molecules of the monomer  
with S configuration 34

### Figure 3.1

22.5 MHz  $^{13}\text{C}$  NMR spectra of the equilibrium



mixture of 1-pyrroline and its trimer 45

Figure 3.2

Plot of the equilibrium constant K vs. the initial concentration of the trimer of 1-pyrroline in CD<sub>3</sub>OD 48

Figure 4.1

Diagram contrasting lone pair - lone pair interactions for the passing (high barrier) and non-passing nitrogen inversion (low barrier), in tetrasubstituted hydrazine ABN-NCD 53

Figure 4.2

A partial diagram for the conformational interconversion in hydrazine ABN-NCD 56

Figure 4.3

Variable temperature <sup>13</sup>C NMR spectra of meso-1,1'-bi(2-methylpiperidine) 63

Figure 4.4

Variable temperature <sup>13</sup>C NMR spectra of meso-1,1'-bi(cis-2,4-dimethylpiperidine) 64

Figure 4.5

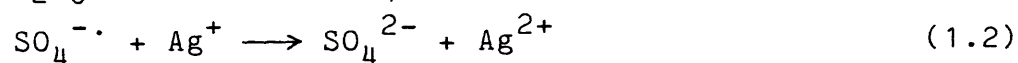
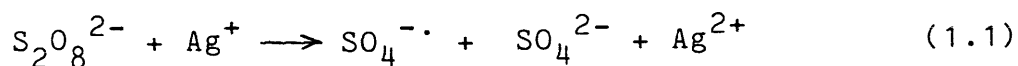
Variable temperature $^{13}\text{C}$ NMR spectra of meso-1,1'-bi(cis-4-tert-butyl-2-methylpiperidine)	65
Figure 4.6 All of the typical gauche and trans conformations in meso-1,1'-bi(2-methylpiperidine)s	69
Figure 4.7 Conformational diagram for meso-1,1'-bi(2-methyl- piperidine)s	71
Figure 4.8 A partial diagram for the conformational interconversion of 1,2-dimethylperhydropyridazine	77
Figure 4.9 Energy profiles of the bond rotation about the C1-C1' bond in meso-1,1'-bi(2-methylcyclohexane), meso-1,1'-bi(cis-2,4-dimethylcyclohexane), meso-1,1'-bi(cis-4-tert-butyl-2-methylcyclo- hexane, and bi(cyclohexane), calculated by MMI as a function of the torsion angle $\omega(\text{H} - \text{C1} - \text{C1}' - \text{H})$	86

## Chapter 1

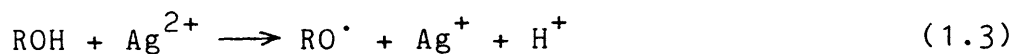
Silver(I)-catalyzed Oxidation of Cyclic Secondary Amines  
with Peroxodisulfate<sup>1)</sup>

## 1.1 Introduction

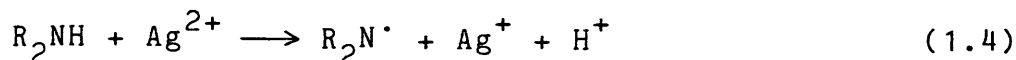
An electron-transfer process in the silver(I)-catalyzed oxidation with peroxodisulfate has recently been recognized.<sup>2-4)</sup> In the presence of silver(I) ion, peroxodisulfate decomposes according to equations (1.1) and (1.2):<sup>5)</sup>



Caronna et al. and Walling et al. revealed that in the silver(I)-catalyzed oxidation of alcohols, silver(II) ion abstracts an electron from the oxygen atom to give alkoxyl radicals [equation (1.3)].<sup>2,3)</sup>



Hence, it is expected that aminyl radicals are generated in the oxidation of amines under alkaline conditions [equation (1.4)].



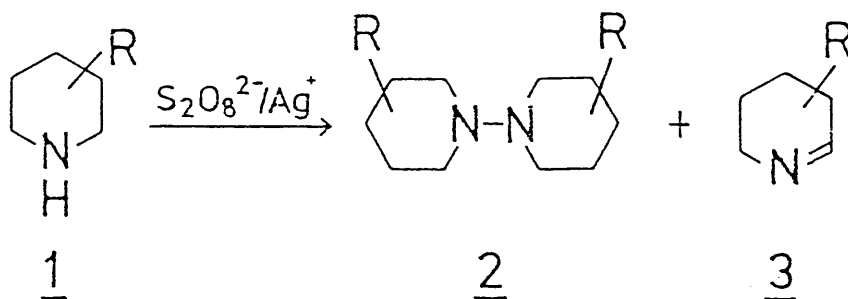
Although Bacon et al. reported that treatment of aliphatic amines with an aqueous alkaline solution of sodium peroxodisulfate in the presence of silver nitrate gave aldehydes or ketones via imine intermediates, the yield being low and variable in the case of secondary amines, they did not refer to the intermediacy of aminyl radicals.<sup>6)</sup> We describe here the silver(I) catalyzed oxidation of cyclic secondary amines with peroxodisulfate, which can be considered to involve aminyl radicals as intermediates.

## 1.2 Results and Discussion

The oxidation of the piperidines (1) gave the 1,1'-bipiperidines (2) [See Table 1.1 (p.3)]. VPC analysis of the ethereal extract of the reaction mixture revealed that 2,3,4,5-tetrahydropyridines (3) were formed as sole by-products, the ratio of 1,1'-bipiperidines (2) to 2,3,4,5-tetrahydropyridines (3) being high (4.9 - 31) except in the case of 2-methylpiperidine (0.6).

Since 2-methylpiperidine (1b) and 3-methylpiperidine (1c) both have an asymmetric center, (+)- and meso-isomers occur in the corresponding 1,1'-bipiperidines. Although the diastereoisomeric mixture of 3,3'-dimethyl-1,1'-bipiperidine

Table 1.1. Silver(I)-catalyzed Oxidation of Piperidines with Peroxodisulfate



Product yield (%) <sup>a, b)</sup>		
<u>1</u> - <u>3</u>	<u>2</u>	<u>3</u>
<u>a</u> (R = H)	48 (61)	(2)
<u>b</u> (R = 2-Me)	dl 5 (9)	(26)
	meso 3 (7)	
<u>c</u> (R = 3-Me)	30 (62) <sup>c)</sup>	(2)
<u>d</u> (R = 4-Me)	24 (39)	(8)
<u>e</u> (R = 4-Ph)	14	

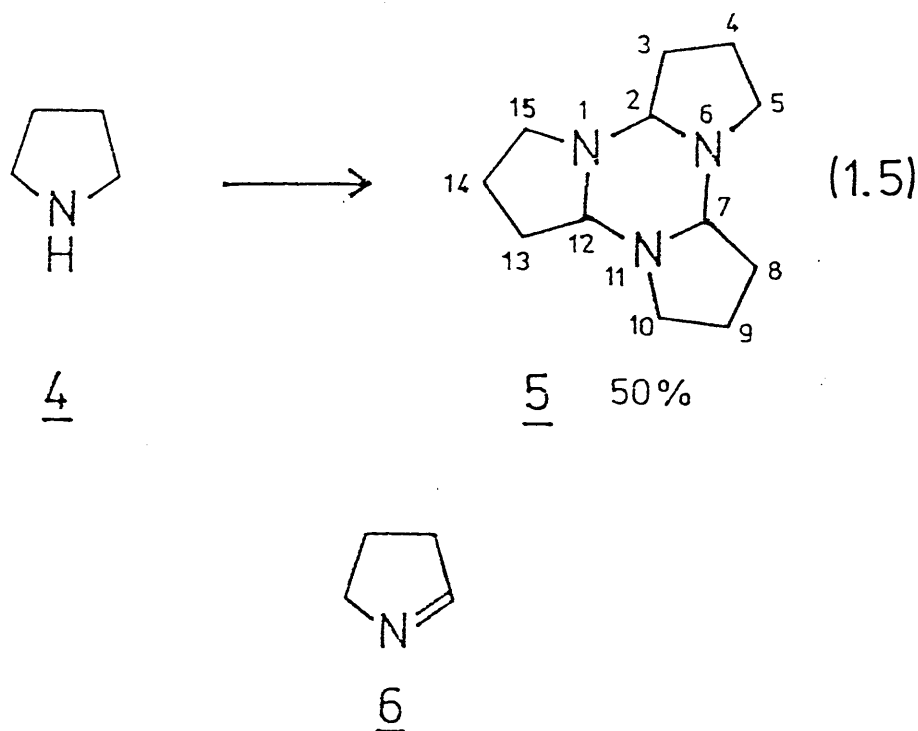
a) Isolated yield. b) Values in parentheses are yield determined by VPC. c) Inseparable diastereoisomeric mixture.

(2c) was inseparable, that of 2,2'-dimethyl-1,1'-bipiperidine (2b) was separated into the (+)- and meso-isomers. Assignment of the diastereoisomers rests on the comparison on VPC and TLC of the optically pure (S,S)-2,2'-dimethyl-1,1'-bipiperidine (S,S)-(2b) ( $[\alpha]_D^{20} +179^\circ$  in EtOH) produced from (S)-2-methylpiperidine (S)-(1b) ( $[\alpha]_D^{20} 36^\circ$  in hexane)<sup>7)</sup> with the two diastereoisomers.

For the 1,1'-bipiperidines, which are interesting compounds in the conformational analysis (See Chapter 4),<sup>8)</sup> preparative methods have only been reported for 1,1'-bipiperidine (2a), and all of these require several tedious and costly steps if one wants to start with piperidines.<sup>9,10)</sup> Furthermore, overall yields obtained by using these known procedures are usually low (at most 10 %). In contrast, our present method involves a very simple preparative procedure which guarantees a high yield (48 %).

The oxidation of pyrrolidine (4) afforded a 1-pyrroline trimer, i.e. 1,6,11-triazatetracyclo[10.3.0.0<sup>2,6</sup>.0<sup>7,11</sup>]-pentadecane (5), exclusively [equation (1.5)]. Its molecular formula was established by elemental analysis and cryoscopic measurements. A mass spectroscopic analysis suggested that it decomposes under the measurement conditions into the corresponding monomer, 1-pyrroline (6). Its <sup>13</sup>C{<sup>1</sup>H} NMR spectrum (CDCl<sub>3</sub>) indicated four peaks at  $\delta$  81.96 (C-2, -7, -12), 45.79 (C-5, -10, -15), 27.96 (C-3, -8,

-13), and 20.37 ppm (C-4, -9, -14) in complete agreement with its apparent  $C_3$  symmetry. The  $^1\text{H}$  off-resonance decoupled  $^{13}\text{C}$  NMR spectrum clearly showed three triplets and a doublet, in accord with the presence of nine methylene and three methine carbons in a molecule with  $C_3$  symmetry\*.




---

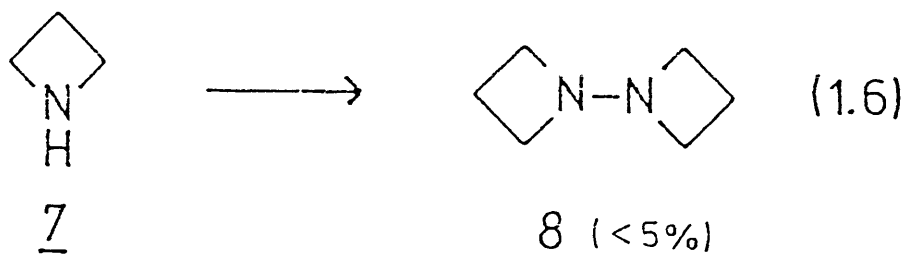
\* If the nitrogen inversion is faster than the NMR time scale, 5 satisfies apparent  $C_3$  symmetry regardless of its conformations, since all three methine protons are considered to be axial by analogy with the conformation of 2,3,4,5-tetrahydropyridine trimer (See Chapter 2).

---

The presence of a proton attached to the  $sp^2$  carbon was precluded by its  $^1H$  NMR spectrum, which showed complex multiplets at  $\delta(CDCl_3)$  3.1 (6 H), 2.4 (3 H), and 1.9 (12 H). Hence, the structure of the trimer is represented by compound 5.

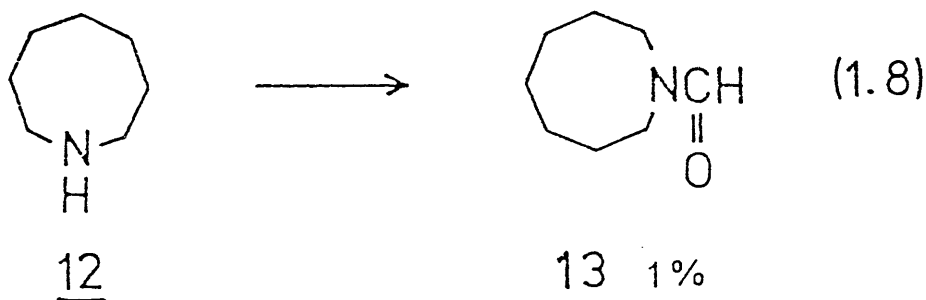
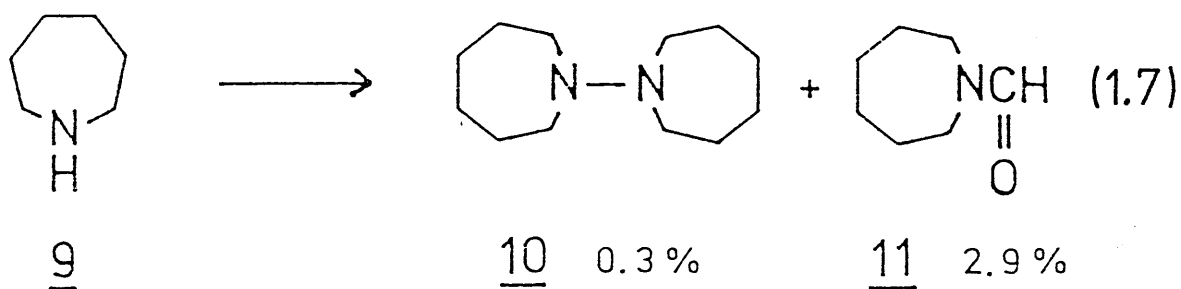
The preparation and the structure of the 1-pyrroline trimer have been ambiguous because of its thermal and acid lability.<sup>11,12)</sup> Although the liquid thought to be the 1-pyrroline trimer was obtained by Fuhlhage and Van der Werf,<sup>12)</sup> it was never isolated in the pure form and its physical properties were not characterized. Thus, the structure of the 1-pyrroline trimer has been established for the first time in the present work.

Oxidation of azetidine (7) gave 1,1'-biazetidine (8) [equation (1.6)] and an uncharacterized compound together with polymeric materials. In spite of various attempts compound 8 could not be isolated without the uncharacterized compound.<sup>\*\*</sup>





Oxidation of perhydroazepine (9) gave 1,1'-biperhydroazepine (10) and 1-formylperhydroazepine (11) [equation (1.7)], together with a large amount of polymeric material. In the oxidation of perhydroazocine (12), 1-formylazocine (13) was the sole isolated product [equation (1.8)] from the ethereal extract of the reaction mixture, a large part of which was polymeric material.




---

\*\* Nelsen et al.<sup>13)</sup> and Kirste et al.<sup>14)</sup> reported the synthesis of compound 8 by a photochemical or a thermal decomposition of 1,1'-azoazetidine. They isolated it by preparative VPC. We tried to isolate it by adapting their conditions (OV-210, column temperature 150 °C), but found that it decomposed on the column.

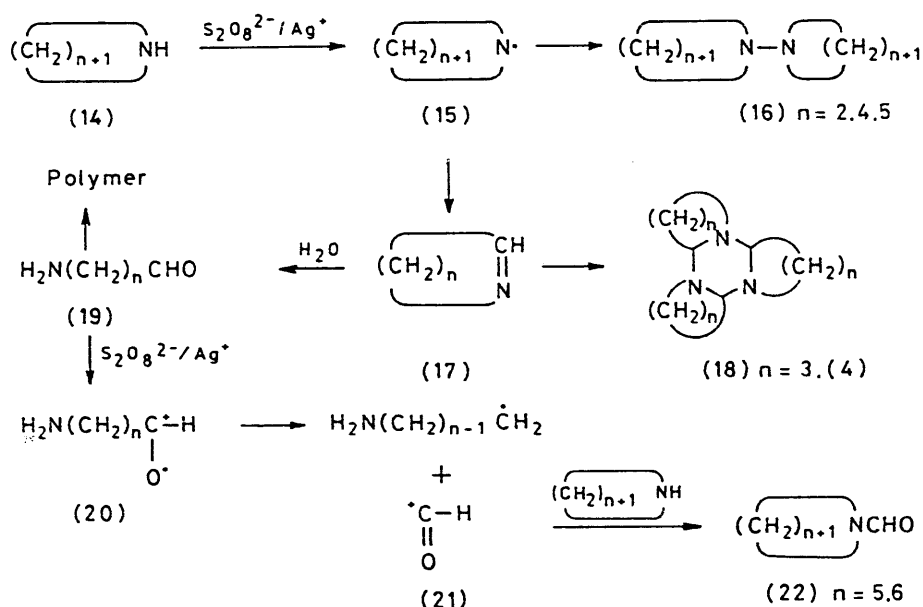
---

It is worth mentioning that N,N-coupling reactions were observed in the oxidation of azetidine (7), the piperidines (1), and perhydroazepine (9). While oxidative N,N-coupling of aromatic secondary amines to the corresponding hydrazines has been accomplished with various agents,<sup>15)</sup> that of aliphatic or cyclic secondary amines has not been observed previously. Thus, our result is the first example of direct N,N-coupling of non-aromatic secondary amines.

Mechanistically, the present reaction may be explained by the assumption that aminyl radicals are involved as intermediates [Figure 1.1 (p.9)]. Since in the absence of silver nitrate 1,1'-bipiperidine was not formed, we consider that the silver(II) ion generated according to equations (1.1) and (1.2) abstracts an electron from the nitrogen atom of a cyclic secondary amine (14) to give an aminyl radicals (15) [See Figure 1.1 and equation (1.4)]. The combination of radicals gives the N,N-coupling products (16), and the hydrogen abstraction from the neighbouring C-H bond affords the cyclic imines (17). While cyclic imines generated from pyrrolidine and from piperidines generally give the corresponding trimers (18),<sup>16)</sup> the cyclic imine from 2-methylpiperidine stands as the monomer (3b), probably for steric reasons.<sup>17)</sup> Cyclic imines formed from perhydroazepine (9) and from perhydroazocine (12) are likely to be hydrolyzed to give amino aldehydes (19). Although such

compounds (19) under the reaction conditions would for the most part undergo intermolecular condensation to give polymers, to some extent further oxidation with  $S_2O_8^{2-} - Ag^+$  occurs to form the radical cation (20) by an electron-transfer process. The radical cation (20) cleaves to give a formyl cation (21) which reacts with the remaining cyclic amine to give the formamide (22). It is worth noticing that the products depend largely on the ring size of the cyclic amines in this reaction.

Figure 1.1. Tentative scheme for the silver(I)-catalyzed oxidation of cyclic secondary amines



### 1.3 Experimental

#### General

60 MHz, 90 MHz, and 100 MHz  $^1\text{H}$  NMR spectra were recorded on JEOL C60-HL, Varian EM-390, and JEOL MH-100 spectrometers, respectively. 15 MHz, 20 MHz, and 22.5 MHz  $^{13}\text{C}$  NMR spectra were recorded on JEOL FX60, Varian CFT-20, and JEOL FX90Q spectrometers, respectively. Mass spectra were measured on a Hitachi RMU-6D mass spectrometer. IR spectra were determined on Jasco DS-430 or A202 grating infrared spectrometers. Vapour phase chromatography (VPC) was conducted in most cases on a JEOL JGC-1100F instrument with a stainless-steel column (2 m x 4 mm, 15 % Triton-X305 on 60 - 80 mesh Uniport B), or a Varian-Aerograph Model 920 with an aluminium column (2 m x 3/8 in., 15 % Triton-X305 on 60 - 80 mesh Uniport B). Occasionally a Shimadzu GC-3BT instrument with a stainless steel column (2 m x 6 mm, 5 % FFAP on 60 - 80 mesh Uniport B) was used. Optical rotations were measured with an automatic Yanaco OR-50 polarimeter by using a quartz cell with a 1.0-cm path length. For the column chromatography, silica gel (C-200, Wako Chemicals), activated alumina powder (200 mesh, Wako Chemicals), or neutral activated alumina powder (WOELM, grade 1) was used. Melting points are uncorrected. Ether refers to diethyl ether throughout.

Oxidation of Piperidine (1a).

A 25 % aqueous solution of sodium peroxodisulfate (11.9 g, 0.05 mol) was added dropwise below 10 °C to a stirred mixture of the piperidine (1a) (4.3 g, 0.05 mol), sodium hydroxide (4.0 g, 0.10 mol), and a catalytic amount of silver nitrate (43 mg, 0.25 mmol) in water (50 mL) and the mixture was then stirred for an additional 2.5 h. After the reaction mixture had been saturated with sodium chloride, it was extracted with ether and the ethereal extract was dried ( $\text{MgSO}_4$ ). Evaporation of the extract under reduced pressure gave an oily residue (2.67 g) which was shown by VPC to contain 1,1'-bipiperidine (2a) (97 %) and the trimer of 2,3,4,5-tetrahydropyridine (3a) (3 %). The residue was chromatographed on a silica-gel column using hexane-ethyl acetate (10 : 1) as eluant, to give compound 2a (2.0 g, 48 %). Evaporative distillation (room temp./0.5 mmHg) gave an analytically pure sample as colorless needles (mp 19.5 - 20.5 °C).  $^1\text{H}$  NMR ( $\text{CDCl}_3$ )  $\delta$  2.9 - 2.7 (8 H, m), and 1.9 - 1.2 (12 H, m);  $^{13}\text{C}$  NMR ( $\text{CDCl}_3$ )  $\delta$  49.31 (t), 26.65 (t), and 24.89 (t); mass spectrum,  $m/e$  168 ( $\text{M}^+$ ). Anal. Calcd for  $\text{C}_{10}\text{H}_{20}\text{N}_2$ : C, 71.37; H, 11.98; N, 16.65. Found: C, 71.29; H, 12.07; N, 16.81.

Picrate: mp 153.5 - 154.0 °C (from  $\text{EtOH-H}_2\text{O}$ , 3 : 2) (lit.,<sup>10</sup>) 153 - 154 °C).

Compound (3a) was identical with an authentic sample by

VPC comparison.<sup>16)</sup>

Oxidation of 2-Methylpiperidine (1b).

A 25 % aqueous solution of sodium peroxodisulfate (71.4 g, 0.3 mol) was added dropwise below 10 °C to a stirred mixture of 2-methylpiperidine (1b) (19.8 g, 0.2 mol), sodium hydroxide (24 g, 0.6 mol), and silver nitrate (1.70 g, 0.01 mol) in water (300 mL) and the mixture was stirred for an additional 2.5 h. After saturation of the reaction mixture with sodium chloride, precipitated inorganic materials were filtered off. The filtrate was extracted with ether and the extract was dried (MgSO<sub>4</sub>). Evaporation of the extract under reduced pressure gave an oily residue (9.6 g), which was shown by VPC to contain (+)-2,2'-dimethyl-1,1'-bipiperidine [(+)-2b] (18 %), meso-2,2'-dimethyl-1,1'-bipiperidine [meso-2b] (14 %), 2,3,4,5-tetrahydro-6-methylpyridine (3b) (55 %), unchanged 2-methylpiperidine (11 %), and uncharacterized materials (2 %). The residue was chromatographed on an alumina column, using hexane as eluant, to give (+)-2b (0.94 g, 5 %) and meso-2b (0.61 g, 3 %), both as colorless oils.

For (+)-2b: bp 70.0 °C at 0.9 mmHg; <sup>1</sup>H NMR (CDCl<sub>3</sub>) δ 2.9 (1 H, m), 2.6 - 2.0 (2 H, m), 1.8 - 1.0 (6 H, m), and 1.02 (3 H, d); <sup>13</sup>C NMR (CDCl<sub>3</sub>) δ 54.53 (d), 43.98 (t), 35.68 (t), 26.87 (t), 25.28 (t), and 20.93 (q); mass spectrum, m/e (70 eV) 196 (M<sup>+</sup>). Anal. Calcd for C<sub>12</sub>H<sub>24</sub>N<sub>2</sub>: C, 73.41; H,

12.32; N, 14.27. Found: C, 73.12; H, 12.51; N, 14.13.

For meso-2b: bp 71.5 °C at 0.9 mmHg;  $^1\text{H}$  NMR ( $\text{CDCl}_3$ )  $\delta$  3.1 - 2.4 (3 H, m), 2.0 - 1.1 (6 H, m), and 1.10 (3 H, d);  $^{13}\text{C}$  NMR (diglyme- $d_{14}$  at 100 °C)  $\delta$  58.38 (d), 48.96 (t), 36.69 (t), 27.74 (t), 24.55 (t), and 20.15 (q);<sup>8)</sup> mass spectrum, m/e (70 eV) 196 ( $\text{M}^+$ ). Anal. Calcd for  $\text{C}_{12}\text{H}_{24}\text{N}_2$ : C, 73.41; H, 12.32; N, 14.27. Found: C, 73.21; H, 12.51; N, 14.13.

Compound 3b was identified by a VPC comparison with an authentic sample.<sup>17)</sup>

(S)-(+)-2-Methylpiperidine [(S)-1b].<sup>7)</sup>

Resolution of a racemic mixture of 2-methylpiperidine with (+)-tartaric acid gave the salt, (+)-2-methylpiperidinium hydrogen tartrate, mp 64 - 65 °C (lit.,<sup>7c)</sup> 65 - 66 °C). On treatment with alkali it was converted into (S)-1b,  $[\alpha]_{\text{D}}^{23.5} +36.4^\circ$  (c 3.46 in hexane) [lit.,<sup>7c)</sup>  $[\alpha]_{\text{D}}^{15} 36.5$  (c 4.90 in hexane)].

(S,S)-(+)-2,2'-Dimethyl-1,1'-bipiperidine [(S,S)-2b].

Oxidation of the (S)-isomer of compound 1b was carried out in the same manner as that of the racemic mixture of 2-methylpiperidine to give (S,S)-2b as colorless oil,  $[\alpha]_{\text{D}}^{20} 179^\circ$  (c 0.454 in EtOH). The peak of (+)-2b in VPC coincided with that of (S,S)-2b. Coincidence between (+)-

(S,S)-2b and 2b spots in TLC was also confirmed.

Oxidation of 3-Methylpiperidine (1c).

3-Methylpiperidine (1c) (9.9 g, 0.1 mol) was oxidized in the same manner as piperidine. The reaction mixture was extracted with dichloromethane and the extract was dried ( $\text{MgSO}_4$ ). Evaporation of the extract under reduced pressure gave an oily residue (6.4 g), which was shown by VPC to contain 3,3'-dimethyl-1,1'-bipiperidine (2c) (93 %) and the trimer of 2,3,4,5-tetrahydro-5 (or 3)-methylpyridine (3c) (3 %). The residue was chromatographed on a silica-gel column, using hexane-ethyl acetate (5 : 1) as eluant, to give (2c) (3.0 g, 30 %) as an inseparable diastereoisomeric mixture in the form of a colorless oil, bp 106 °C / 17 mmHg;  $^1\text{H}$  NMR ( $\text{CDCl}_3$ )  $\delta$  3.1 - 2.8 (4 H, m), 2.7 - 1.2 (14 H, m), and 0.9 (6 H, d);  $^{13}\text{C}$  NMR ( $\text{CDCl}_3$ )  $\delta$  57.04 (t), 56.65 (t), 48.63 (t), 48.27 (t), 33.47 (t), 31.97 (d), 25.81 (t), and 19.74 (q); mass spectrum, m/e (70 eV) 196 ( $\text{M}^+$ ). Anal. Calcd for  $\text{C}_{12}\text{H}_{24}\text{N}_2$ : C, 73.41; H, 12.32; N, 14.27. Found: C, 73.27; H, 12.31; N, 13.99.

Identification of compound 3c was based on a VPC comparison with a specimen, which was prepared by treatment of 1-chloro-3-methylpiperidine with alkali (KOH-MeOH). In the  $^{13}\text{C}$  NMR spectrum of the specimen, all the signals (ca. 76 peaks) appeared at higher than 88 ppm. Its  $^1\text{H}$  NMR



spectrum showed the absence of a proton attached to the  $sp^2$  carbon. Hence, the specimen is not the monomer of 2,3,4,5-tetrahydro-3(or 5)-methylpyridine, but it is probably an isomeric mixture of the trimers of 2,3,4,5-tetrahydro-3(or 5)-methylpyridine.

Oxidation of 4-Methylpiperidine (1d).

4-Methylpiperidine (1d) (5.0 g, 0.05 mol) was oxidized in the same manner as piperidine 1a. The reaction mixture was extracted with ether, dried ( $MgSO_4$ ), and concentrated under reduced pressure to give an oily residue (2.6 g), which was shown by VPC to contain 4,4'-dimethyl-1,1'-bipiperidine (2d) (83 %) and 2,3,4,5-tetrahydro-4-methylpyridine (3d) (17 %). The residue was chromatographed on a silica-gel column using hexane-ethyl acetate (9 : 1) as eluant to give 2d (1.18 g, 24 %). Evaporative distillation (50 °C/0.5 mmHg) gave an analytically pure sample as a colorless oil which solidified in the receiver, mp 27.0 - 28.0 °C, bp 63 °C / 0.5 mmHg;  $^1H$  NMR ( $CDCl_3$ )  $\delta$  2.9 - 2.7 (4 H, m), 2.5 - 2.2 (4 H, m), 1.8 - 1.0 (10 H, m), and 0.88 (6 H, d);  $^{13}C$  NMR ( $CDCl_3$ )  $\delta$  48.34 (t), 34.84 (t), 31.23 (d), and 21.72 (q); mass spectrum, m/e (70 eV) 196 ( $M^+$ ). Anal. Calcd for  $C_{12}H_{24}N_2$ : C, 73.41; H, 12.32; N, 14.27. Found: C, 73.69; H, 12.37; N, 14.21.

Picrate: mp 148.5 - 149.5 °C, needles (from MeOH).

Anal. Calcd for  $C_{12}H_{24}N_2 \cdot C_6H_3N_3O_7$ : C, 50.82; H, 6.40; N, 16.46. Found: C, 51.08; H, 6.50; N, 16.58.

Identification of compound 3d was based on a VPC comparison with a specimen. For the synthesis and structural confirmation, see Chapter 2.

Oxidation of 4-Phenylpiperidine (1e).

A 25 % aqueous solution of sodium peroxodisulfate (3.52 g, 15 mmol) was added dropwise at room temperature to a stirred mixture of 4-phenylpiperidine (1e) (1.61 g, 10 mmol), sodium hydroxide (2.0 g, 50 mmol), silver nitrate (85 mg, 0.05 mmol), water (100 mL), and acetonitrile (25 mL) (necessary to dissolve 1e), and the mixture was stirred for an additional 2.5 h. After the reaction mixture had been saturated with sodium chloride, it was extracted with ether and the dried ( $MgSO_4$ ) extract was concentrated under reduced pressure to give a residue (1.44 g). A few mL of ethanol was added and the precipitate was collected and washed with ethanol to give a spectroscopically pure sample of 4,4'-diphenyl-1,1'-bipiperidine (2e) (235 mg, 15 %) as colorless crystals. It was dissolved in dichloromethane, filtered through a short column of activated alumina, and rinsed with dichloromethane. Evaporation of dichloromethane and crystallization of the residue from ethanol gave analytically pure compound 2e as colorless prisms, mp 195.0

- 196.0 °C;  $^1\text{H}$  NMR ( $\text{CDCl}_3$ )  $\delta$  7.6 - 7.2 (10 H, m), and 3.4 - 3.2 (18 H, m);  $^{13}\text{C}$  NMR ( $\text{CDCl}_3$ )  $\delta$  146.22 (s), 128.38 (d), 126.87 (d), 126.09 (d), 48.90 (t), 43.05 (d), and 33.98 (t); mass spectrum, m/e (70 eV) 320 ( $\text{M}^+$ ). Anal. Calcd for  $\text{C}_{22}\text{H}_{28}\text{N}_2$ : C, 82.45; H, 8.81; N, 8.74. Found: C, 82.27; H, 9.06; N, 8.85.

#### Oxidation of Pyrrolidine (4).

A 25 % solution of sodium peroxodisulfate (35.7 g, 0.15 mol) was added dropwise below 10 °C to a stirred mixture of pyrrolidine (4) (10.6 g, 0.15 mol), sodium hydroxide (12 g, 0.3 mol), and silver nitrate (127 mg, 0.75 mmol) in water (150 mL) and the mixture was stirred for 2.5 h. The reaction mixture was then saturated with sodium chloride, extracted with dichloromethane, and the extract was dried ( $\text{MgSO}_4$ ) and concentrated under reduced pressure on an ice-bath. Ether (ca. 15 mL) was added and the precipitate was filtered off. The filtrate was evaporated under reduced pressure at 0 °C to give the almost pure 1-pyrroline trimer (5) (5.3 g, 50 %) as a faint orange oil, which was found to be of satisfactory purity for NMR spectra. Elution of the product through a neutral alumina column with ether followed by evaporation of the ether afforded an analytically pure sample of 5 as a colorless oil. IR (neat)  $2790\text{ cm}^{-1}$  (Bohlmann band<sup>18</sup>);  $^1\text{H}$  NMR ( $\text{CDCl}_3$ )  $\delta$  3.2 - 3.0 (6 H, m), 2.5

- 2.1 (3 H, m), and 2.1 - 1.2 (12 H, m);  $^{13}\text{C}$  NMR ( $\text{CDCl}_3$ )  $\delta$  81.96 (d), 45.79 (t), 27.96 (t), and 20.37 (t); mass spectrum,  $m/e$  (70 eV) 71 ( $\text{M}^+$  of 1-pyrroline). Molecular weight, obtained by cryoscopic measurement of a benzene solution, was 229 ( $\text{C}_{12}\text{H}_{21}\text{N}_3$  requires 209). Anal. Calcd for  $\text{C}_{12}\text{H}_{21}\text{N}_3$ : C, 69.52; H, 10.21; N, 20.27. Found: C, 69.22; H, 10.51; N, 20.06.

#### Oxidation of Perhydroazepine (9).

A 25 % aqueous solution of sodium peroxodisulfate (59.5 g, 0.25 mol) was added dropwise below 10 °C to a stirred mixture of perhydroazepine (9) (19.8 g, 0.20 mol), sodium hydroxide (20.0 g, 0.5 mol), and silver nitrate (1.70 g, 0.05 mol) in water (250 mL) and the mixture was stirred for 17 h. After saturation of the reaction mixture with sodium chloride, the precipitated materials were filtered off. The filtrate was extracted with dichloromethane and the dried ( $\text{MgSO}_4$ ) extract was concentrated under reduced pressure. The residue, most of which was polymer-like material, was distilled by Kugel-Rohr (100 - 150 °C/1 mmHg) to give a colorless oil. VPC separation afforded 1,1'-biperhydroazepine (10) (0.13 g, 0.3 %) and 1-formylperhydroazepine (11) (0.74 g, 2.9 %), both as colorless oils.

For 10:  $^1\text{H}$  NMR ( $\text{CDCl}_3$ )  $\delta$  2.8 - 2.6 (8 H, m) and 1.7 -

1.5 (16 H, m);  $^{13}\text{C}$  NMR ( $\text{CDCl}_3$ )  $\delta$  52.06 (t), 28.39 (t), and 26.65 (t); mass spectrum,  $m/e$  196 ( $\text{M}^+$ ). Anal. Calcd for  $\text{C}_{12}\text{H}_{24}\text{N}_2$ : C, 73.41; H, 12.32; N, 14.27. Found: C, 73.60; H, 12.30; N, 14.08.

For 11: Bp 60.5 - 61.0 °C/0.5 mmHg; IR (neat) 1650  $\text{cm}^{-1}$  (amido C=O); its IR spectrum was superimposable upon that reported for N-formylperhydroazepine;<sup>19)</sup>  $^1\text{H}$  NMR ( $\text{CDCl}_3$ )  $\delta$  8.12 (1 H, s), 3.6 - 3.4 (4 H, m), and 1.9 - 1.5 (8 H, m);  $^{13}\text{C}$  NMR ( $\text{CDCl}_3$ )  $\delta$  162.83 (d), 47.67 (t), 43.48 (t), 30.25 (t), 27.95 (t), 26.96, and 26.87; mass spectrum,  $m/e$  (70 eV) 127 ( $\text{M}^+$ ). Anal. Calcd for  $\text{C}_7\text{H}_{13}\text{NO}$ : C, 66.10; H, 10.30; N, 11.02. Found: C, 65.90; H, 10.38; N, 10.97.

#### Oxidation of Perhydroazocine (12).

A 25 % aqueous solution of sodium peroxodisulfate (11.4 g, 48 mmol) was added dropwise below 10 °C to a stirred mixture of perhydroazocine (12) (4.52 g, 40 mmol), sodium hydroxide (4.8 g, 120 mmol), silver nitrate (34 mg, 0.2 mmol), and acetonitrile (12 mL) in water (50 mL) and the mixture was stirred for 7 h. The reaction mixture was then saturated with sodium chloride and extracted with ether. The dried ( $\text{MgSO}_4$ ) extract was evaporated and the residue, most of which was polymer-like material, was distilled by Kugel-Rohr (120 °C/0.5 mmHg). Preparative VPC of the distillate gave 1-formylperhydroazocine (13) as a colorless

oil (52 mg, 1 %). Its NMR and IR spectra were superimposable upon those of the authentic sample which was prepared in the following manner.

Authentic Sample of 1-Formylperhydroazocine (13).

A mixture of perhydroazocine (12) (3.28 g, 29 mmol) and ethyl formate (11 g, 149 mmol) was refluxed for 1 h. Evaporation under reduced pressure gave an oily residue (4.2 g). Kugel-Rohr distillation (100 °C/0.5 mmHg) of the residue (2.1 g) afforded compound 13 as a colorless oil (1.3 g, 64 %). IR (neat) 1675 - 1665  $\text{cm}^{-1}$  (amido C=O);  $^1\text{H}$  NMR ( $\text{CDCl}_3$ )  $\delta$  8.1 (1 H, s), 3.5 - 3.2 (4 H, m), and 1.9 - 1.3 (10 H, m);  $^{13}\text{C}$  NMR ( $\text{CDCl}_3$ )  $\delta$  162.90 (d), 49.10 (t), 43.93 (t), 27.30, 26.91, 25.84, and 24.57; mass spectrum, m/e (70 eV) 141 ( $\text{M}^+$ ). Anal. Calcd for  $\text{C}_8\text{H}_{15}\text{NO}$ : C, 68.04; H, 10.71; N, 9.92. Found: C, 67.90; H, 10.90; N, 9.63.

Oxidation of Azetidine (7).

Azetidine<sup>20)</sup> (7.06 g, 124 mmol) was oxidized in a similar manner to piperidine. The dried ( $\text{Na}_2\text{SO}_4$ ) ethereal extract was evaporated under reduced pressure to give an oily residue (0.565 g), which was shown by NMR to contain 1,1'-biazetidine (8), as the main component and an uncharacterized compound A as a minor component along with some impurities. Although the impurities were removed by a

Kugel-Rohr distillation (80 °C/0.5 mmHg), various attempts to separate 8 from A were unsuccessful. The structure of 8 was elucidated by comparison of the  $^1\text{H}$  NMR spectra with the reported spectrum<sup>13)</sup> as well as on the basis of the  $^{13}\text{C}$  NMR spectra;  $^1\text{H}$  NMR ( $\text{CDCl}_3$ )  $\delta$  3.20 (8 H, t,  $J=7$  Hz) and 2.00 (4 H, quintet,  $J=7$  Hz);  $^{13}\text{C}$  NMR ( $\text{CDCl}_3$ )  $\delta$  49.80 (t) and 14.38 (t).

## 1.4 References

- 1) Nomura,Y.; Ogawa,K.; Takeuchi,Y.; Tomoda,S., Chem.Lett., 1977, 693; *ibid.*, 1978, 271. Ogawa,K.; Nomura,Y.; Takeuchi,Y.; Tomoda,S., J.Chem.Soc., Perkin Trans. 1., 1982, 3031.
- 2) Caronna,T.; Citterio,A.; Grossi,L.; Minisci,F.; Ogawa,K., Tetrahedron, 1976, 32, 2741.
- 3) Walling,C.; Camaioni,D.M., J.Org.Chem., 1978, 43, 3266.
- 4) (a) Clerici,A.; Minisci,F.; Ogawa,K.; Surzur,J.M., Tetrahedron Lett., 1978, 1149. (b) Clerici,A.; Porta,O., J.Chem.Soc., Perkin Trans. 2, 1980, 1234. (c) Citterio,A., Gazz.Chim.Ital., 1980, 110, 253. (d) Minisci,F.; Citterio,A.; Giordano,C., Acc.Chem.Res., 1983, 16, 27.
- 5) House,D.A., Chem.Rev., 1962, 62, 185.
- 6) (a) Bacon R.G.R.; Stewart, D., J.Chem.Soc., C, 1966, 1384. (b) Bacon R.G.R.; Hanna,W.J.W.; Stewart,D., J.Chem.Soc., C, 1966, 1388.
- 7) (a) Ladenburg,A., Justus Liebigs Ann.Chem., 1888, 247, 1. (b) Marckwald,W., Ber., 1896, 29, 43. (c) Leithe,W., Monatsh.Chem., 1928, 50, 40. (d) Craig,J.C.; Buckingham,J., "Atlas of Stereochemistry", Chapman and Hall Ltd., London, 1974, p.14.
- 8) (a) Ogawa,K.; Takeuchi,Y.; Suzuki,H.; Nomura,Y., Chem.Lett., 1981, 697. (b) Ogawa,K.; Takeuchi,Y.;



- Suzuki, H.; Nomura, Y., J.Chem.Soc., Chem. Commun., 1981, 1015. (c) Ogawa, K.; Takeuchi, Y.; Suzuki, H.; Nomura, Y., J.Am.Chem.Soc., in press.
- 9) (a) Rink, M.; Lux, R., Naturwissenschaften, 1958, 45, 516. (b) Rink, M.; Mehta, M.; Lux, R., Arch.Pharm.(Weinheim, Ger.), 1961, 294, 640. (c) Nelsen, S.F.; Weisman, G.R., Tetrahedron Lett., 1973, 2321. (d) Kauffmann, T.; Albrecht, J.; Berger, D.; Legler, J., Angew.Chem., Int.Ed.Engl., 1967, 6, 633.
- 10) Mackay, D.; Waters, W.A., J.Chem.Soc., C, 1966, 813.
- 11) Schöpf, C.; Oechler, F., Justus Liebigs Ann.Chem., 1936, 523, 1.
- 12) Fuhlhage, D.W.; Van der Werf, C.A., J.Am.Chem.Soc., 1958, 82, 6249.
- 13) Nelsen, S.F.; Peacock, V.E.; Weisman, G.R.; Landis, M.E.; Spencer, J.A., J.Am.Chem.Soc., 1978, 100, 2806.
- 14) Kirste, K.; Luttke, W.; Rademacher, P., Angew.Chem., Int.Ed.Engl., 1978, 17, 680.
- 15) (a) Wieland, H.; Gambarjan, S., Ber., 1906, 39, 1499. (b) Neugebauer, F.A.; Fischer, P.H.H., Chem.Ber., 1965, 98, 844. (c) Ram, N.; Sidhu, K.S., Indian J.Chem., Sect. A, 1978, 16, 195. (d) Kajimoto, T.; Takahashi, H.; Tsuji, J., Bull.Chem.Soc.Jpn., 1982, 55, 3673.
- 16) (a) Schöpf, C.; Komzak, A.; Braun, F.; Jacobi, E., Justus Liebigs Ann.Chem., 1948, 559, 1. (b) Schöpf, C.; Arm, H.;

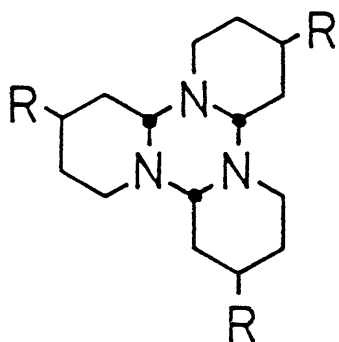
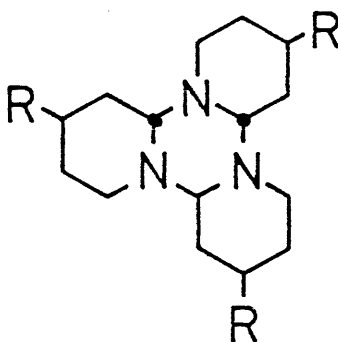
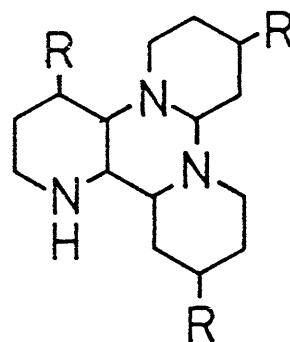
- Krimm, H., Chem. Ber., 1951, 84, 690.
- 17) Grundon M.F.; Reynolds, B.E., J. Chem. Soc., 1963, 3898;  
ibid., 1964, 2445.
- 18) Bohlmann, F., Chem. Ber., 1958, 91, 2157.
- 19) Pouchert, C.J., "The Aldrich Library of Infrared Spectra", Second Edn., Aldrich Chemical Co., Wisconsin, 1975, F1655-9, p.394-c.
- 20) Wadsworth, D.H., Org. Syntheses, 1973, 53, 13.

## Chapter 2

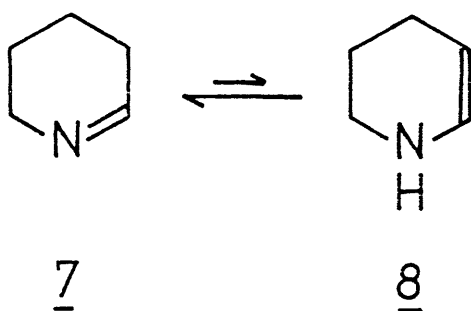
Conformational Analysis of the Trimer of  
2,3,4,5-Tetrahydro-4-methylpyridine

## 2.1 Introduction

2,3,4,5-Tetrahydropyridines, which were formed as the by-products in the silver(I)-catalyzed oxidation of piperidines with peroxodisulfate (See Chapter 1),<sup>1)</sup> have interesting properties. Schöpf et al. found that three isomeric trimers of 2,3,4,5-tetrahydropyridine  $\alpha$ (1),  $\beta$ (2) and iso (3) were formed by dehydrochlorination of 1-chloropiperidine.<sup>2)</sup>

R=H : 1R=Me : 42536

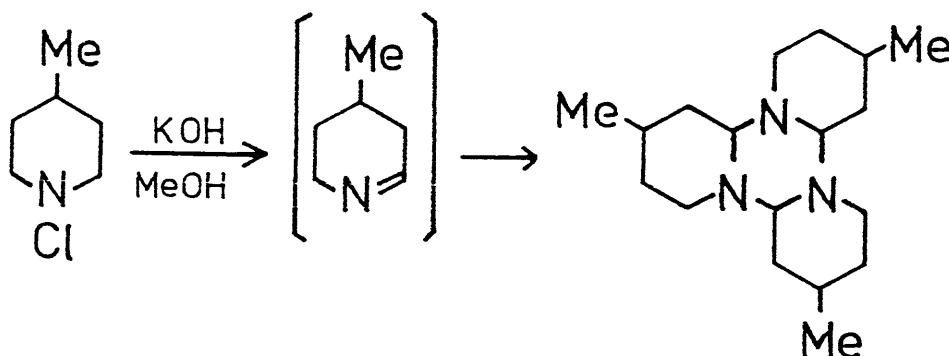
The  $\alpha$  isomer, the major product in the dehydrochlorination of 1-chloropiperidine under the usual condition, results from the  $\pi_s^2 + \pi_s^2 + \pi_s^2$  cycloaddition of the cyclic azomethine (7). The  $\beta$  isomer results from the  $\pi_s^2 + \pi_s^2 + \pi_a^2$  cycloaddition. There are three asymmetric methine carbons in  $\alpha$  and  $\beta$  isomers. The  $\alpha$  isomer is a racemic mixture of RRR and SSS chirality, and has  $C_3$  symmetry. The  $\beta$  isomer is a racemic mixture of RRS and SSR chirality, and has  $C_1$  symmetry. The iso isomer results from the cycloaddition of two molecules of 7 and one molecule of the cyclic enamine (8), the tautomer of 7, and is a constitutional isomer of the  $\alpha$  and  $\beta$  isomers.



Kessler et al. established the configurations and the conformations of these isomers by  $^{13}\text{C}$  NMR.<sup>3)</sup> We describe here the conformational analysis of the trimer of 2,3,4,5-tetrahydro-4-methylpyridine with the aid of  $^{13}\text{C}$  NMR and molecular mechanics calculation.

## 2.2 Results and Discussion

Dehydrochlorination of 1-chloro-4-methylpiperidine by potassium hydroxide in methanol gave a yellow oil (9) in 73% yield.<sup>4)</sup>



Crystallization of it from acetone gave colorless crystals 10 (mp 61.5 - 63.0 °C). Its molecular formula was determined to be  $(C_6H_{11}N)_3$  by elemental and mass spectroscopic analyses. In the mass spectrum of 10, the molecular ion peak ( $M^+$  291) was observed with the relative intensity of 0.1 % to the base peak ( $m/e$  55). High resolution mass spectrum of 10 are summarized in Table 2.1 (p.28). Observation of the fragment ions of 2-aza-1,3-butadiene and propene suggests that 2,3,4,5-tetrahydro-4-methylpyridine monomer (11), generated by the decomposition of its trimer under the measurement condition, was further decomposed according to the equation (2.1) (retro Diels-Alder reaction).

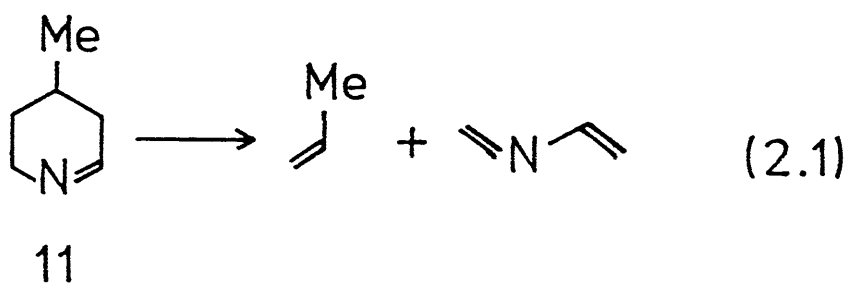


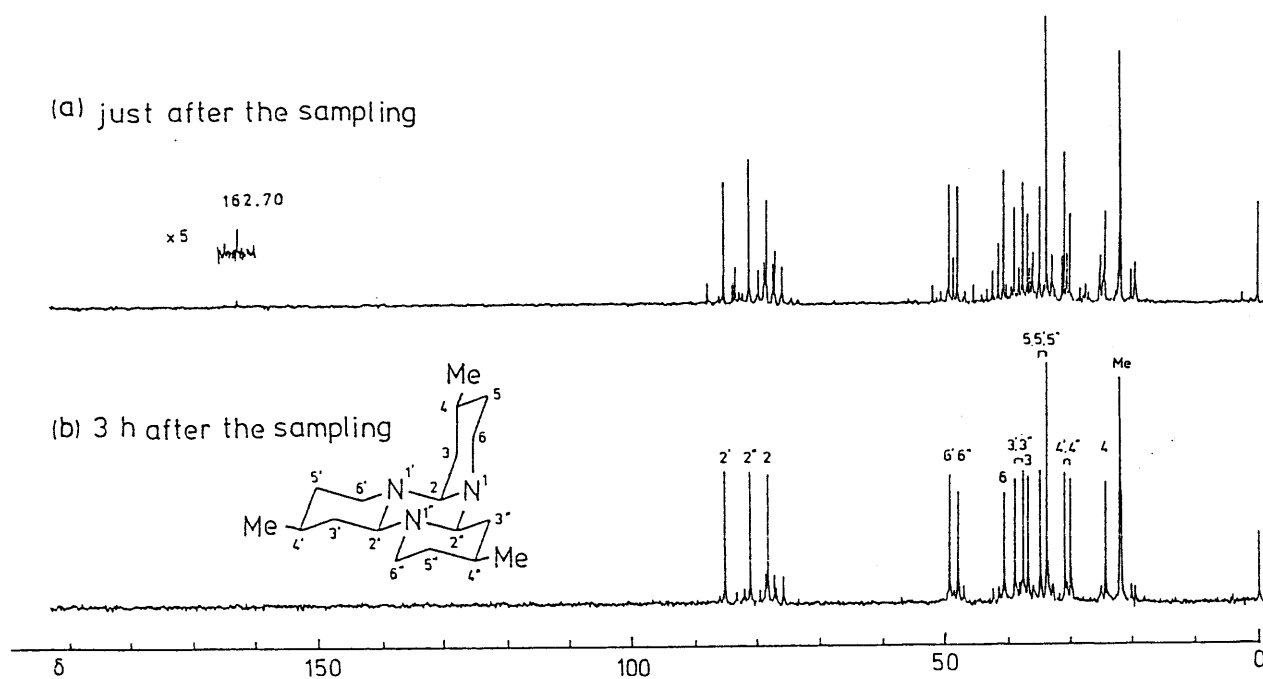
Table 2.1. Major Fragment Ions of the Trimer of 2,3,4,5-Tetrahydro-4-methylpyridine in High Resolution Mass Spectroscopy

No.	m/e Obsd.	Error <sup>a)</sup>	Unsat.	Composition	Assignable structure
1	42.0440	-2.8	1.0	C <sub>3</sub> H <sub>6</sub>	
2	55.0434	1.2	2.0	C <sub>3</sub> H <sub>5</sub> N	
3	82.0694	3.7	2.5	C <sub>5</sub> H <sub>8</sub> N	
4	97.0900	0.8	2.0	C <sub>6</sub> H <sub>11</sub> N	

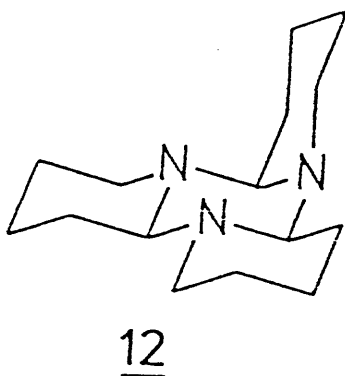
a) Error = (Obsd - Calcd) × 1000

Its IR spectrum did not show the absorption for C=N or N-H bond. Its <sup>13</sup>C{<sup>1</sup>H} NMR spectrum obtained at 3 h after the sampling showed strong peaks for 18 carbons together with ca. 20 weak peaks [Figure 2.1.b (p.29)].

Figure 2.1. 22.5 MHz  $^{13}\text{C}$  NMR of the trimer of 2,3,4,5-tetrahydro-4-methylpyridine in  $\text{CDCl}_3$ . (a) just after the sampling. (b) 3 h after the sampling.



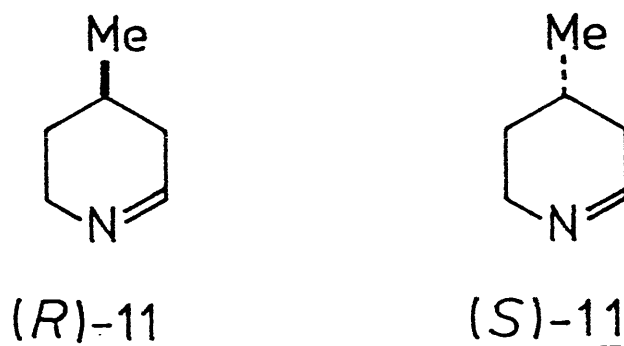
According to Kessler et al., in the most stable conformation of the  $\alpha$  isomer 1 all of the methine hydrogens of the perhydro-1,3,5-triazine ring are axial and one of the nitrogen-bound methylenes is equatorial (12).<sup>3)</sup>



In view of this fact, the most stable conformer of the trimer of 2,3,4,5-tetrahydro-4-methylpyridine should be aeeee in Figure 2.2 (p.32). In this figure are shown all of the conformers interconvertible by that inversion process which involves a nitrogen inversion and the concomitant inversion of the piperidine ring with the inverted nitrogen. Although each of the conformers has the corresponding enantiomer, only one of the enantiomers is depicted. Nomenclature of the conformers in Figure 2.2 [as well as Figure 2.3 (p.34)] are made as follows: The first descriptor e (a) indicates that N1-CH<sub>2</sub> is equatorial (axial)



to the perhydro-1,3,5-triazine ring. The second descriptor e(a) indicates that 4-methyl group is equatorial (axial) to the piperidine ring. Similarly, the third, the fourth, the fifth, and the sixth descriptor indicate the orientation of N1'-CH<sub>2</sub>, 4'-Me, N1''-CH<sub>2</sub>, and 4''-Me, respectively. The calculated <sup>13</sup>C chemical shifts for aeeeee, which were obtained by the approach of Kessler et al. for 1 and 2, agree well with the <sup>13</sup>C chemical shifts of the strong peaks in Figure 2.1.b [See Table 2.2 (p.33)].



Since C4 in the monomer 11 is an asymmetric center, two types of combinations are possible in its trimerization. The first one is the combination of three molecules of (R)-11 ((S)-11). The second one is the combination of the two molecules of (R)-11 ((S)-11) and one molecule of (S)-11 ((R)-11).

Figure 2.2. Conformational interconversion in the trimer of 2,3,4,5-tetrahydro-4-methylpyridine formed by the combination of one molecule of the monomer with R configuration [(R)-11] and two molecules of the monomers with S configuration [(S)-11].

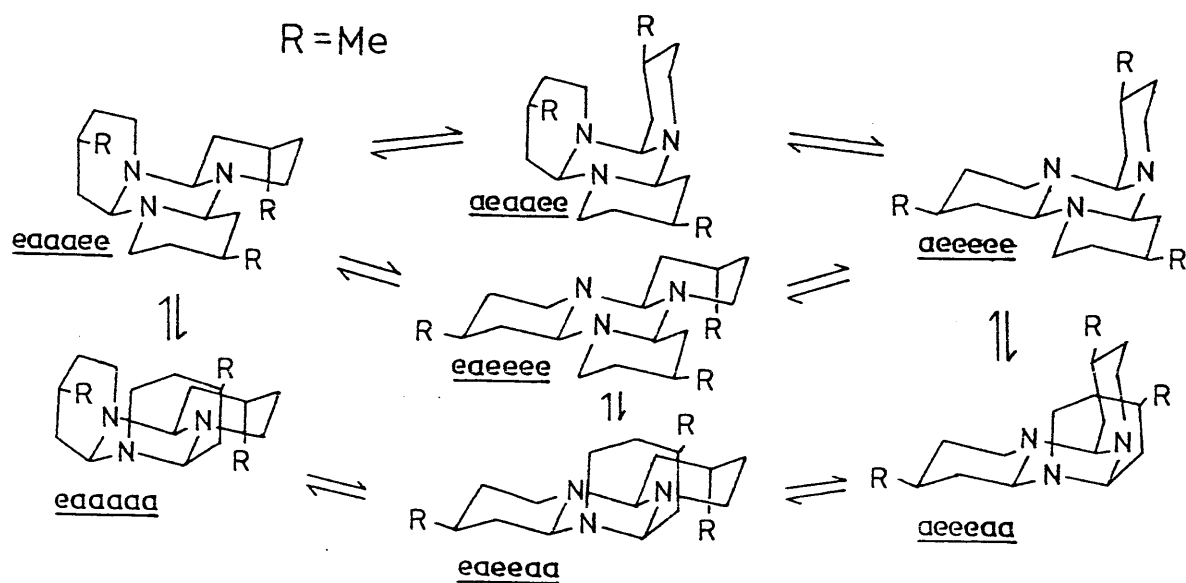


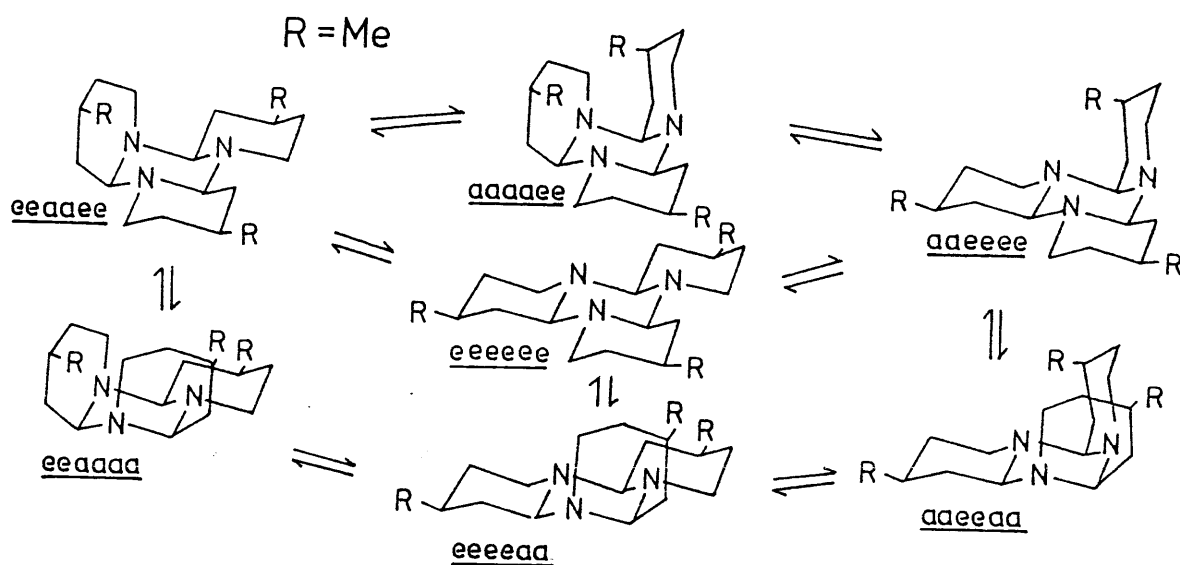
Table 2.2. Observed and Calculated  $^{13}\text{C}$  Chemical Shifts for the Trimer of 2,3,4,5-Tetrahydro-4-methylpyridine

$\delta$		Position
Obsd. <sup>a)</sup>	Calcd. <sup>b)</sup>	
85.03	82.87	2'
80.98	80.19	2"
78.15	77.52	2
49.24	47.98	6' } c)
47.87	47.98	6" }
40.61	39.33	6
38.85	37.05	3' } c)
37.54	37.05	3" }
34.86	34.53	3
36.76	35.03	5 }
33.78	35.03	5' } c)
33.78	35.03	5" }
30.91	28.96	4' } c)
29.98	28.96	4" }
24.37	23.56	4
22.13		4-Me }
22.13		4'-Me } c)
21.94		4"-Me }

a) In  $\text{CDCl}_3$ .    b) See the text.    c)

Relative assignments uncertain.

Figure 2.3. Conformational interconversion in the trimer of 2,3,4,5-tetrahydro-4-methylpyridine formed by the combination of three molecules of the monomer with S configuration [(S)-11].



We name here the trimer of 11 in which all of the methine hydrogens of the perhydro-1,3,5-triazine ring are axial (4) as the  $\alpha$  isomer, analogously to 1. Conformational interconversions in the  $\alpha$  isomer formed by the first combination are shown in Figure 2.3. A conformer eeeeee has  $C_3$  symmetry. By a nitrogen inversion and the concomitant inversion of the piperidine ring which has the inverted nitrogen, eeeeee is interconvertible with one of three equivalent conformers aaeeee, eeaaee, and eeeeaa. The interconversion among these conformers is also possible through one of three equivalent conformers aaaaee, eeaaaa, and aaeeaa. All of the conformers in Figure 2.3 have an apparent  $C_3$  symmetry under the condition that the inversion processes are fast on the time scale of NMR. Since aaaaee, eeaaaa, and aaeeaa must be considerably less stable than other conformers, it is expected that  $^{13}\text{C}$  NMR of the  $\alpha$  isomer formed by the first combination of the monomer 11 should show one or two sets of six peaks at high temperatures. However, such a spectrum was not observed.

The trimer formed by the second combination is asymmetric. In the conformer aeaeae (Figure 2.2), the configurations of  $C_4$ ,  $C_4'$ , and  $C_4''$  are R, S, and S, respectively (i.e. the second combination), and all of the configurations of  $C_2$ ,  $C_2'$ , and  $C_2''$  are S. Hence it is concluded that a stereoselective trimerization of 11

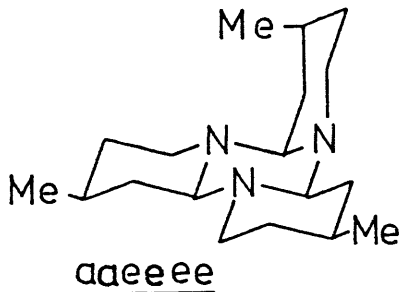
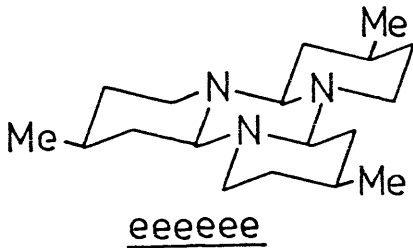
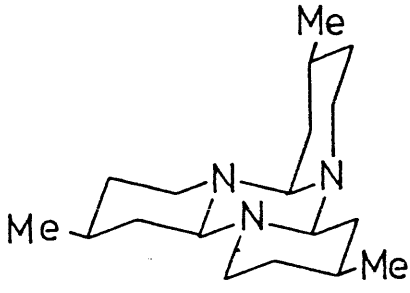
occurred after a selective combination of two molecules of (S)-11 ((R)-11) and one molecule of (R)-11 ((S)-11).

$^{13}\text{C}$  NMR spectrum of the colorless crystals 10 in chloroform-d measured just after the sampling showed many weak signals in addition to the strong signals for aeeeee (Figure 2.1.a). Noticeably the signal assignable to the azomethine carbon of 11 was observed at  $\delta$  162.70. Most of those weak signals disappeared after 3 h to give the spectrum shown in Figure 2.1.b. The  $^{13}\text{C}$  NMR spectrum obtained at 24 h after the sampling was identical with Figure 2.1.b. The  $^{13}\text{C}$  NMR spectrum of the oil 9 in chloroform-d measured at 24 h after the sampling was also superimposable to Figure 2.1.b. Therefore, aeeeee is the most stable structure of the trimer of 11 in chloroform-d. Most of the weak signals in Figure 2.1.a and 2.1.b may be assigned to the constitutional isomers 5 and 6, corresponding to the  $\beta$  (2) and iso (3) isomers, respectively, and to the monomer 11.

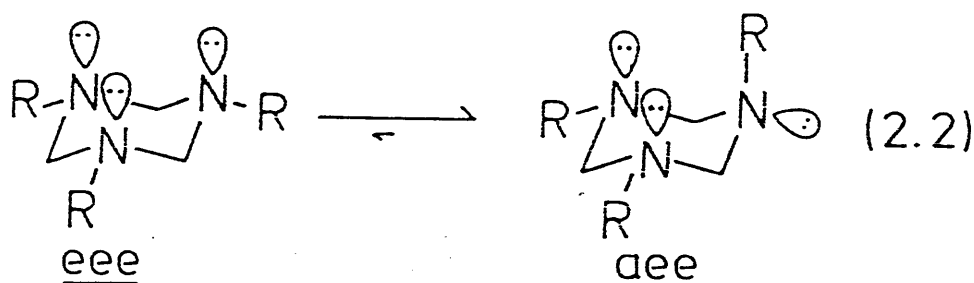
Since the spectrum changes from Figure 2.1.a to Figure 2.1.b, it seems that the structure of the trimer in the solid phase might be different from that in chloroform-d solution. The most stable structure aeeeee should occur by the trimerization after a dissociation of 10 to the monomer 11.

Table 2.3. Molecular Mechanics Calculation of the Trimers of 2,3,4,5-Tetrahydro-4-methylpyridine

MMI Calculation

Combination	Conformation	Steric Energy / kcal mol <sup>-1</sup>
<u>SSS</u> ( <u>RRR</u> )	 <u>aaeeee</u>	3.75
	 <u>eeeeee</u>	2.77
<u>RSS</u> ( <u>SRR</u> )	 <u>aaeeee</u>	0.00

Our conclusion that aeeeee is the most stable structure of the trimer of 11 is also confirmed by molecular mechanics calculation MMI<sup>6)</sup> [See Table 2.3 (p.37)]. The calculation also shows that eeeeee is more stable than aeeeee. It is well known that in 1,3,5-trialkylperhydro-1,3,5-triazine the conformation eee [in equation (2.2)] which has three equatorial N-alkyl groups is less stable than the conformation aee which has one axial and two equatorial N-alkyl groups. This was ascribed to the repulsive electronic interaction between the nitrogen lone pairs parallel to each other.<sup>5)</sup> Our calculation shows that in aeeeee the 1,3-diaxial interaction between the axial methyl group and one of the C-N bonds in the perhydro-1,3,5-triazine ring is so large that the electronically unfavored conformation eeeeee becomes more stable.



The conformer eeeeee has a symmetry number of 3 and is not degenerated when we consider only one set of the



enantiomers. As a result, the free energy of eeeeee  $G_e$  is  $H_e + RT\ln 3$ , where  $H_e$  is the enthalpy of eeeeee. Because of the three-fold degeneracy, the free energy of the mixture of aaeeee, eeaaee, and eeeeaa is  $H_a - RT\ln 3$ , where  $H_a$  is the enthalpy of aaeeee. Hence, the calculated free energy difference between the mixture of aaeeee, eeaaee, and eeeeaa, and eeeeee is given by  $H_a - H_e - 2RT\ln 3 = 0.98 - 4.366 \times 10^{-3} \times T \text{ kcal mol}^{-1}$ . Thus, the free energy of eeeeee is higher than that of the mixture of aaeeee, eeaaee, and eeeeaa by  $0.11 \text{ kcal mol}^{-1}$  at 200 K. Accordingly, it is expected that eeeeee might be observed by NMR at 200 K if the optically pure 11s are trimerized.

### 2.3 Experimental

High resolution mass spectra were measured on a JEOL D300 mass spectrometer.

Preparation of the Trimer of 2,3,4,5-Tetrahydro-4-methylpyridine.

1-Chloro-4-methylpiperidine was prepared according to the method analogous to 1-chloropiperidine.<sup>2,4,7)</sup> To a rapidly stirred suspension of N-chlorosuccinimide (14.0 g, 0.104 mol) in ether (100 mL) was added 4-methylpiperidine (9.9 g, 0.1 mol) under argon on an ice bath. When the addition was complete, the ice bath was removed. After 18 h the mixture was filtered and the filtrate was washed twice with water (50 mL) and once with aqueous sodium chloride (50 mL) and dried ( $\text{MgSO}_4$ ). Evaporation of this ether solution of 1-chloro-4-methylpiperidine under atmospheric pressure below 60 °C of the bath temperature gave the residue (24.67 g) which still contained ether. The residue (22.67 g) was added dropwise over a period of 0.5 h to a stirred solution of KOH (11.2 g, 0.2 mol) in dry MeOH (100 mL) heated at the reflux temperature. After the addition, the mixture was further stirred for 2.5 h at the same temperature and the precipitated KCl was filtered off at the room temperature. The solvent of the filtrate was evaporated under atmospheric pressure at 90 °C of the bath temperature. To the residue

water (80 mL) and ice were added. The solution was extracted with ether. The extract was dried ( $\text{MgSO}_4$ ) and was evaporated under reduced pressure to give a yellow oil 9 (6.5 g; yield 73 % based on 4-methylpiperidine). Crystallization of oil from acetone gave colorless prisms (10), mp 61.5 - 63.0 °C.

Anal. Calcd for  $(\text{C}_6\text{H}_{11}\text{N})_3$ : C, 74.17; H, 11.41; N, 14.42. Found: 74.02; H, 11.32; N, 14.32.

## 2.4 References and Notes

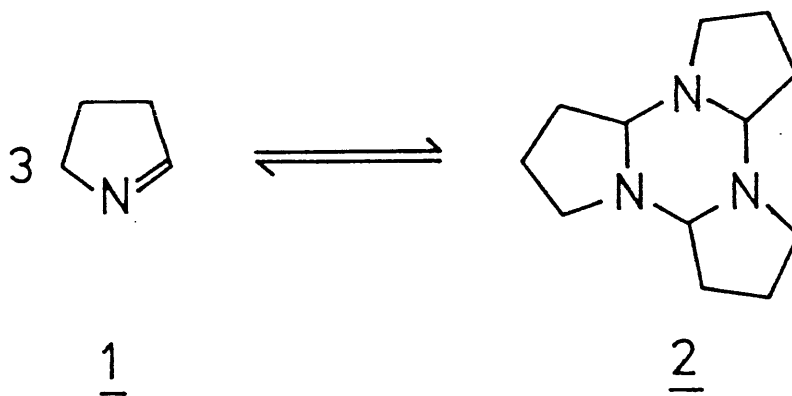
- 1) Nomura,Y.; Ogawa,K.; Takeuchi,Y.; Tomoda,S., Chem.Lett., 1978, 271. Ogawa,K.; Nomura,Y.; Takeuchi,Y.; Tomoda,S., J.Chem.Soc., Perkin Trans.1, 1982, 3031.
- 2) Schöpf,C.; Komzak,A.; Braun,F.; Jacob,E., Justus Liebigs Ann.Chem., 1948, 559, 1. Schöpf,C.; Arm,H.; Krimm,H., Chem.Ber., 1951, 84, 690.
- 3) Kessler,H.; Mohlrle,H.; Zimmermann,G., J.Org.Chem., 1977, 42, 66.
- 4) Grundon,M.F.; Reynolds,B.E., J.Chem.Soc., 1964, 2445. Although they prepared the trimer of 2,3,4,5-tetrahydro-4-methylpyridine as an oil by the similar procedure, they did not fully characterize it.
- 5) For a review of the conformational analysis of perhydro-1,3,5-triazines, see Riddell,F.G., "The Conformational Analysis of Heterocyclic Compounds"; Academic Press: London, 1980; Chapter 5.
- 6) Allinger,N.L., Quantum Chemistry Program Exchange, Indiana University, 1975, Program 318. For our local version, see Chapter 4.
- 7) Quick,J.; Oterson,R., Synthesis, 1976, 745. Claxton,G.; Allen,L.; Grisar,J.M., Org.Syntheses, 1977, 56, 118.

## Chapter 3

 $^{13}\text{C}$  and  $^1\text{H}$  NMR Study of 1-Pyrroline

## 3.1 Introduction

1-Pyrroline (1), which is one of the simple cyclic imines, has remained for a long time as an elusive species because of its lability.<sup>1)</sup> Recently, Poisel reported a  $^1\text{H}$  NMR spectrum of the reaction mixture of the dehydrochlorination of 1-chloropyrrolidine by sodium methoxide in methanol and tert-butyl alcohol, in which the signals for 1 were observed together with the strong signals for the solvents.<sup>2)</sup> He also showed that the trimer (2) of 1 partially decomposed into the monomer 1 during distillation and that the equilibrium between the monomer and the trimer took place in a methanol- $\text{d}_4$  solution of the distillate of 2.

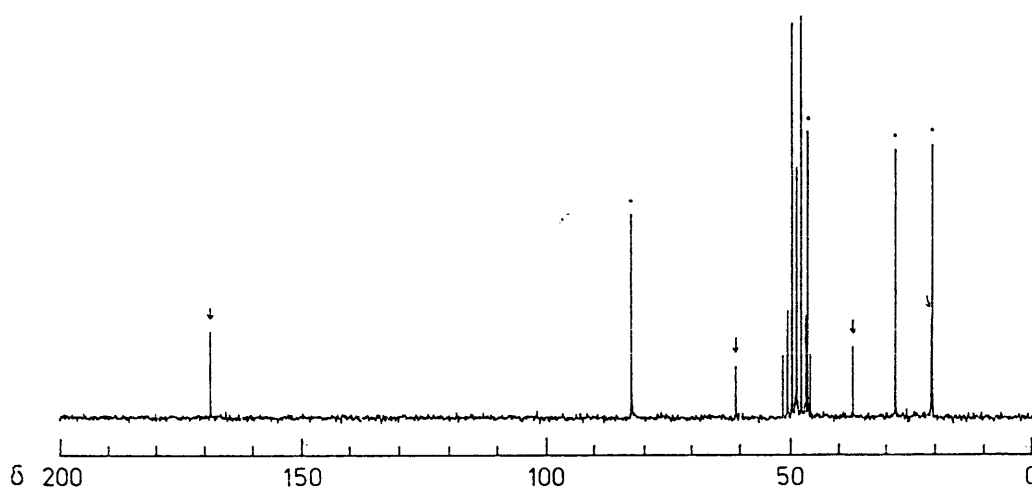


## 3.2 Results and Discussion

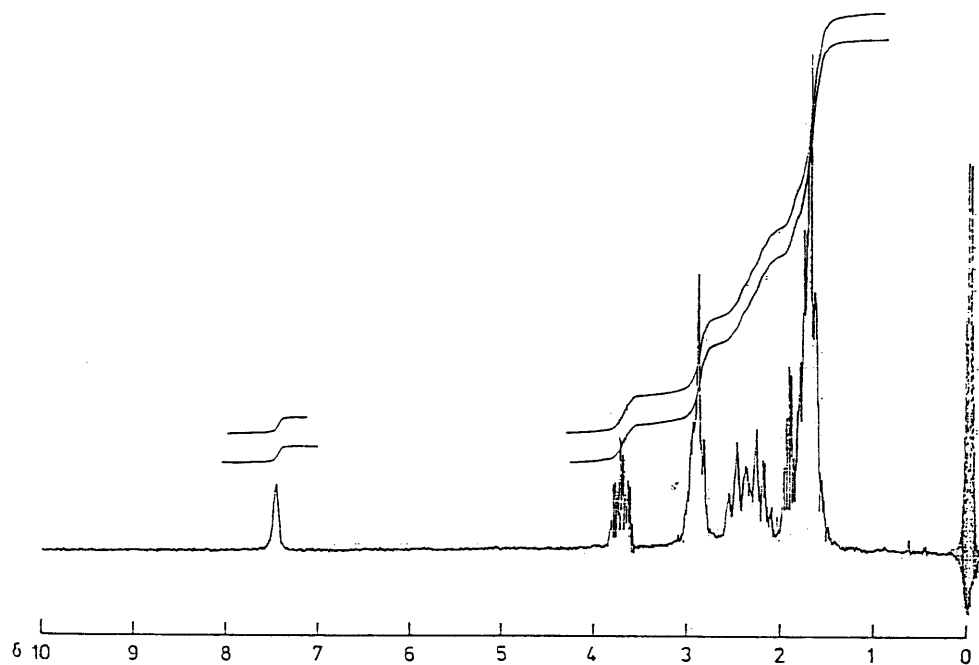
We have found by  $^{13}\text{C}$  and  $^1\text{H}$  NMR that the equilibration occurs between the trimer (2) and the monomer (1) on dissolving the pure 2<sup>3)</sup> in methanol- $\text{d}_4$ , acetonitrile- $\text{d}_3$ , or deuterium oxide [See Figure 3.1 (p.45)]. The  $^{13}\text{C}$  NMR spectrum of the methanol- $\text{d}_4$  solution of the trimer 2 (Figure 3.1.a) showed four weak signals at  $\delta$  169.56, 61.21, 37.21, and 21.12, in addition to four strong signals ( $\delta$  82.88, 46.48, 28.49, and 20.91) due to the trimer 2 and the signal (septet) due to  $\text{CD}_3\text{OD}$ . The weak signal of  $\delta$  169.56, which showed doublet in the  $^1\text{H}$  off-resonance decoupling, was clearly assigned to the azomethine carbon (C2) of the monomer 1. The weak signals of 61.21 and 37.21, both of which showed triplets in the  $^1\text{H}$  off-resonance decoupling, were assigned to C5 and C3 of 1, respectively. The signal of  $\delta$  21.12 was assigned to C4 of 1. The  $^1\text{H}$  NMR spectrum (Figure 3.1.b) showed a signal at  $\delta$  7.50 assigned to the azomethine proton of 1 and a complex multiplet at  $\delta$  3.8 - 3.6 assigned to the nitrogen-bonded methylene protons of 1. The patterns of these signals coincide with those in the  $^1\text{H}$  NMR spectrum of 1 reported by Poisel.

Figure 3.1.

a) 22.5 MHz  $^{13}\text{C}$  NMR spectrum of the equilibrium mixture of 1-pyrroline (1) and the trimer (2) of 1-pyrroline in  $\text{CD}_3\text{OD}$  measured in the gated-decoupling (without NOE) mode. The signal marked by  $\downarrow$  was assigned to 1 and the signal marked by  $\bullet$  was assigned to 2.



b) 90 MHz  $^1\text{H}$  NMR spectrum of the equilibrium mixture of 1 and 2 in  $\text{CD}_3\text{CN}$ .

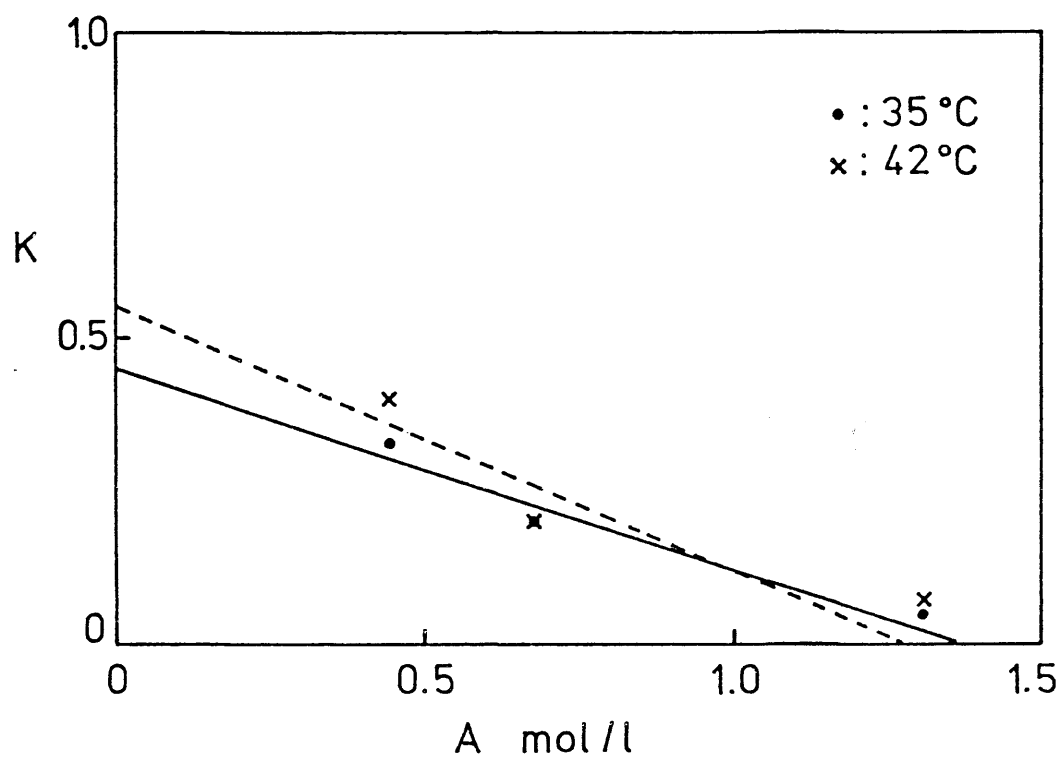




The equilibrium constant  $K = [\underline{1}]_{eq}^3 / [\underline{2}]_{eq}$ , in which  $[\underline{1}]_{eq}$  and  $[\underline{2}]_{eq}$  are the equilibrium concentrations of 1 and 2, respectively, is given by  $K = 9B^3A^2 / (B+3)^2$  where  $B = [\underline{1}]_{eq} / [\underline{2}]_{eq}$  and  $A$  is the initial concentration of 2. The molar ratio  $B$  was determined from the integrated intensities of the appropriate signals in the  $^{13}\text{C}$  NMR spectrum measured in the gated-decoupling (without NOE) mode. The observed  $K$ 's were plotted for the initial concentration of 2 in Figure 3.2 (p.48), which shows that  $K$  strongly depends on  $A$  and the temperature. The more dilute the solution is, the further the equilibrium shifts to the monomer side. The equilibrium constant  $K$  also depends on the solvent. The equilibrium was not observed in benzene- $\text{d}_6$  or THF- $\text{d}_8$  by NMR.

The trimer 2 has often been used as the generator of the monomer 1 in organic synthesis.<sup>4)</sup> Our results would serve as a guide in the choice of the conditions of synthetic reactions utilizing 2. It is also worth mentioning that the  $^{13}\text{C}$  NMR data of 1 in the present work is the first one of those of simple cyclic imines.

Figure 3.2. Plot of the equilibrium constant  $K$  vs. the initial concentration ( $A$ ) of the trimer (2) of 1-pyrroline in  $\text{CD}_3\text{OD}$ .



## 3.3 Experimental

The preparation of 2 was previously reported (See Chapter 1).<sup>3)</sup>

Variable temperature  $^{13}\text{C}$  NMR spectra (22.5 MHz) were recorded on a JEOL FX90Q spectrometer fitted with a variable temperature controller JEOL NM-VTS. All of the  $^{13}\text{C}$  NMR samples were freeze-thaw degassed and sealed in 10 mm od sample tubes. The spectrometer setting for the  $^{13}\text{C}$  NMR measurements in the gated-decoupling (without NOE) mode was the following: Spectral width, 5000 Hz; number of data points, 16 K; pulse angle,  $45^\circ$ ; pulse delay, 40 sec. The observed K's are summarized in Table 3.1, from which Figure 3.2 was made.

Table 3.1. The equilibrium constant K in  $\text{CD}_3\text{OD}$  solution

		A/mol L <sup>-1</sup>		
t/°C		0.4444	0.6735	1.296
42	B	1.72	0.91	0.38
	K	0.406	0.201	0.073
35	B	1.58	0.91	0.34
	K	0.334	0.201	0.053

## 3.4 References

- 1) Schöpf, C.; Oechler, F., Justus Liebigs Ann. Chem., 1936, 523, 1. Mann, P.J.G.; Smitheis, W.R., Biochem.J., 1955, 61, 89. Fuhlhage, D.W.; Van der Werf, C.A., J.Am.Chem.Soc., 1958, 80, 6249. Clarke, A.J.; Mann, P.J.G., Biochem.J., 1959, 71, 596.
- 2) Poisel, H., Monatsh.Chem., 1978, 109, 925.
- 3) See Chapter 1. Nomura, Y.; Ogawa, K.; Takeuchi, Y.; Tomoda, S., Chem.Lett., 1977, 693. Ogawa, K.; Nomura, Y.; Takeuchi, Y.; Tomoda, S., J.Chem.Soc., Perkin Trans.1, 1982, 3031.
- 4) Goldschmidt, B.M., J.Org.Chem., 1962, 27, 4057. Bender, D.R.; Bjeldane, L.F.; Knapp, D.R.; Rapoport, H., J.Org.Chem., 1975, 40, 1264. Petrillo Jr, E.W.; Spitzmiller, E.R., Tetrahedron Lett., 1979, 4929. Cragg, J.E.; Hedges, S.H.; Herbert, R.B., Tetrahedron Lett., 1981, 22, 2127. Kraus, A.G.; Neuenschwander, K., J.Org.Chem., 1981, 46, 4791. Fukawa, H.; Terao, Y.; Achiwa, K.; Sekiya, M., Chem.Lett., 1982, 231.

## Chapter 4

Barriers to Rotation and Inversion  
in meso-1,1'-Bi(2-methylpiperidine)s<sup>1)</sup>

## 4.1 Introduction

Conformational analysis of hydrazines has attracted the interest of physical and organic chemists for more than three decades.<sup>2)</sup> Its static aspects have been investigated extensively. It is established that in a simple acyclic alkylhydrazine both of the nitrogen atoms are pyramidal and that in the most stable conformation of such a hydrazine the lone pairs are gauche to each other.<sup>3-5)</sup> Its dynamic aspects, however, still lack the elucidation of fundamental problems, one of which is concerned with the energy barrier to nitrogen inversions and that to rotations about the N-N bond.<sup>2,6)</sup>

Jones, Katritzky and co-workers have discovered that there are two types of nitrogen inversions, a passing N-inversion (an inversion which involves eclipsing of one pair of substituents in the transition state) and a non-passing N-inversion (an inversion which does not involve eclipsing of substituents).<sup>7)</sup> The high energy barrier in 1,2-dimethylperhydropyridazines ( $\Delta G^\ddagger \approx 12 \text{ kcal mol}^{-1}$ )<sup>8)</sup> has been interpreted in terms of the passing N-inversion, and the low

energy barrier in 1,2-dimethylperhydropyridazines<sup>8)</sup> and acyclic alkylhydrazines 1, 2, and 3 ( $\Delta G^\ddagger \simeq 7 \sim 8$  kcal mol<sup>-1</sup>)<sup>9)</sup> have been interpreted in terms of the non-passing N-inversions.<sup>7)</sup> Originally this barrier difference was attributed to the presence or absence of the alkyl substituents passing. Later Nelsen and Weisman pointed out that the barrier difference should be attributed to the difference in the magnitude of the interaction of the lone pairs in the transition state between the two N-inversions.<sup>10)</sup> While in the transition state of a passing N-inversion two lone pairs are approximately parallel to each other causing a large repulsive interaction which results in a high barrier; in the transition state of a non-passing N-inversion two lone pairs are approximately orthogonal to each other resulting in a low barrier [See Figure 4.1 (p.53)].

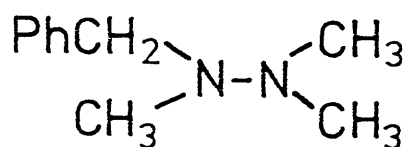
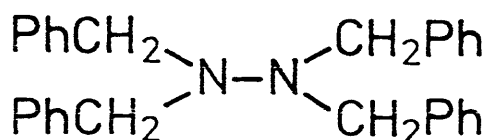
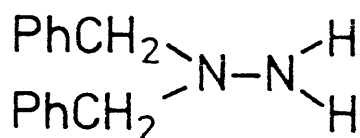
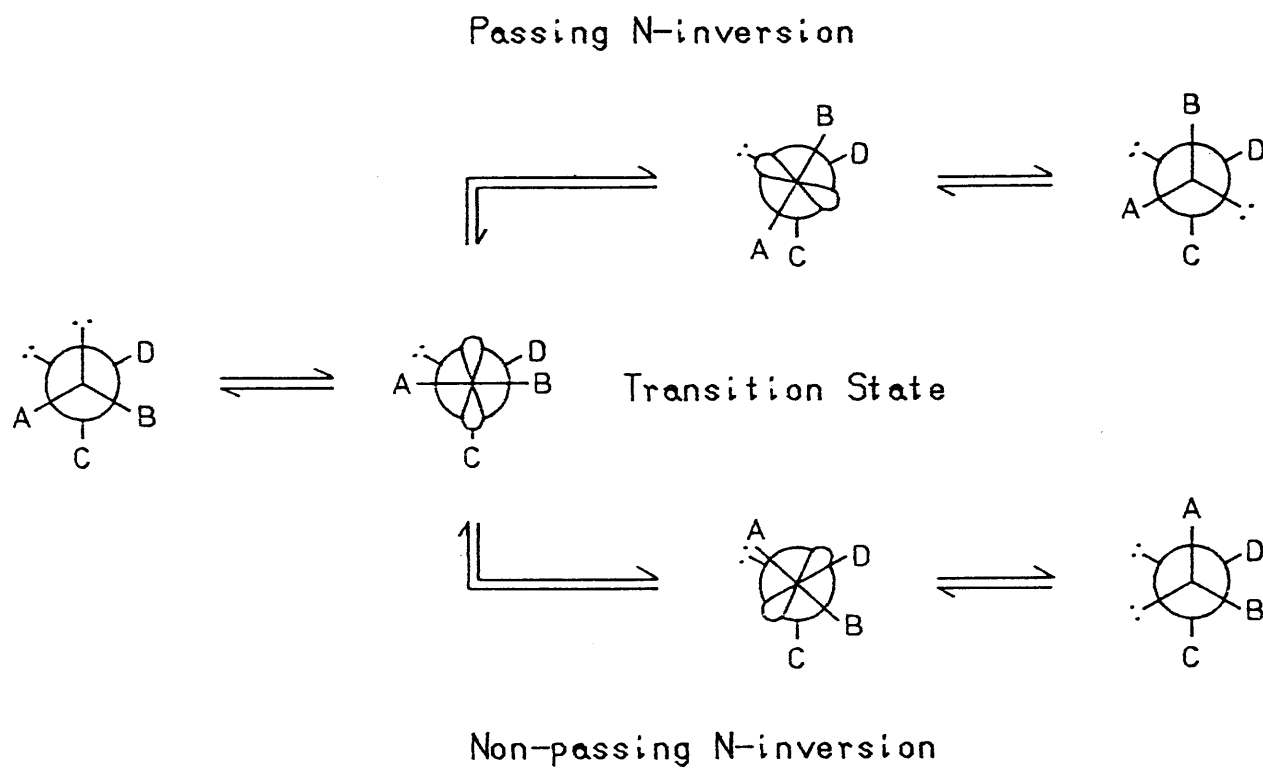
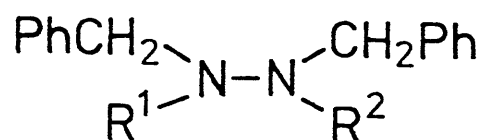
123

Figure 4.1. Diagram contrasting lone pair - lone pair interactions for the passing (high barrier) and for the non-passing nitrogen inversion (low barrier), in tetra-substituted hydrazine  $\begin{smallmatrix} A > N < C \\ B > N < D \end{smallmatrix}$ .



Shvo classified the rotation about the N-N bond into two types, a single-passing rotation (a rotation which involves eclipsing of only one pair of substituents in the transition state) and a double-passing rotation (a rotation which involves eclipsing of two pairs of substituents).<sup>11)</sup> While in the transition state of a double-passing rotation a passing of lone pairs occurs, in a single-passing rotation a passing of lone pairs does not occur. It is expected that the barrier to a double-passing rotation should be substantially higher than that to a single-passing rotation. This expectation has been supported by an infrared and a microwave spectroscopic study of methylhydrazine<sup>12)</sup> and theoretical studies.<sup>13)</sup> Rotational barriers of bipyramidal hydrazines other than methylhydrazine have never been determined unambiguously.



4:  $\text{R}^1 = \text{R}^2 = \text{Et}$

5:  $\text{R}^1 = \text{R}^2 = \text{iso-Pr}$

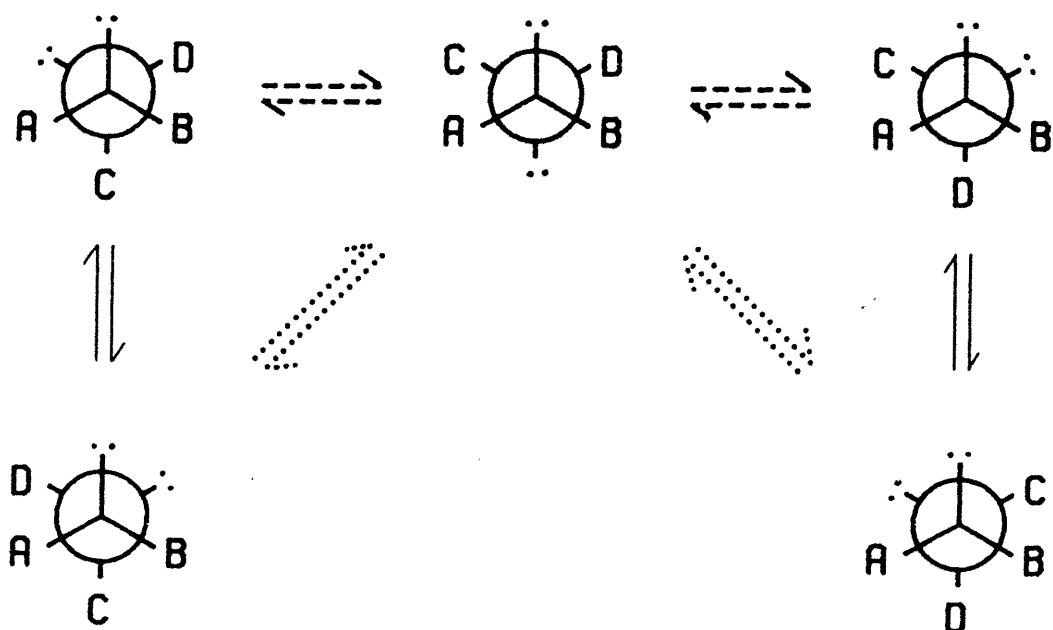
6:  $\text{R}^1 = \text{CH}_2\text{Ph}, \text{R}^2 = \text{Et}$



Fletcher and Sutherland found the free energy barriers of 10.7 - 11.2 kcal mol<sup>-1</sup> for the conformational interconversion in tetraalkylhydrazines 4, 5, and 6 by <sup>1</sup>H NMR. They assigned these barriers to the "rotation" about the N-N bond.<sup>14)</sup> Jones, Katritzky, and co-workers<sup>7)</sup> and Shvo<sup>2)</sup>, however, have pointed out that the reported barriers can be accounted for by assigning them to the passing N-inversion, as well as by assigning them to the single-passing rotation. The two alternative processes have hitherto never been differentiated in acyclic hydrazines in solution. The difficulty in the differentiation between the two alternatives is that they can bring about the same net conformational interconversion through the same trans conformation as the net result [See Figure 4.2 (p.56)].

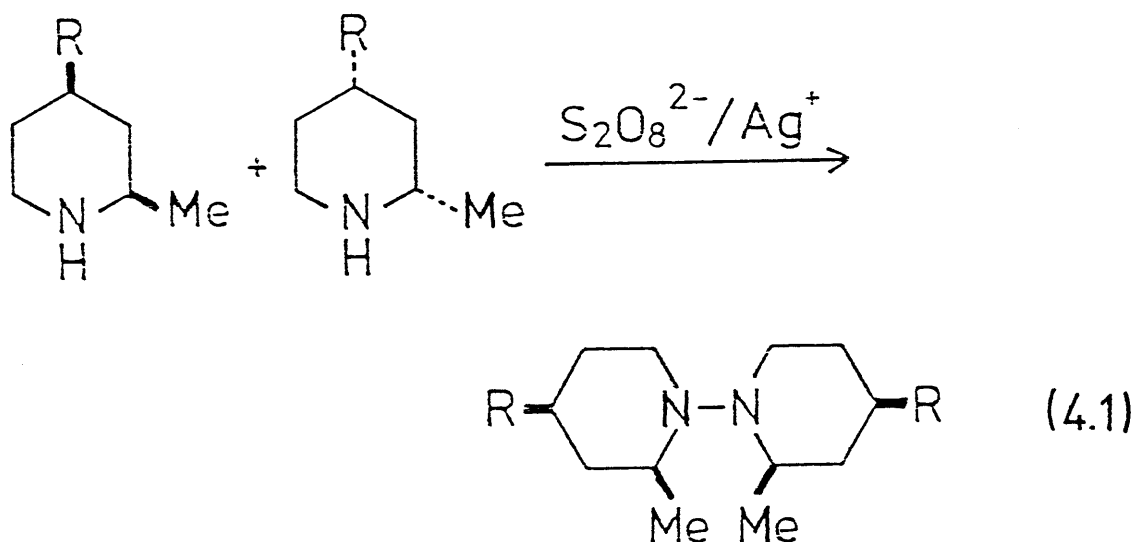
We describe here the first successful differentiation between the two alternatives in meso-1,1'-bi(2-methylpiperidine) (7), meso-1,1'-bi(cis-2,4-dimethylpiperidine) (8), and meso-1,1'-bi(cis-4-tert-butyl-2-methylpiperidine) (9), which leads to the estimation of the barrier to the single-passing rotation, with the aid of <sup>13</sup>C DNMR of these compounds and of molecular mechanics calculations of the corresponding hydrocarbons.

Figure 4.2. A partial diagram for the conformational interconversion in tetrasubstituted hydrazine  $\begin{smallmatrix} A & & C \\ & \backslash & / \\ & N-N & \\ & / & \backslash \\ B & & D \end{smallmatrix}$ . A light, a broken, and a dotted arrow represent a non-passing N-inversion, a passing N-inversion, and a single-passing rotation, respectively.



## 4.2 Synthesis of Materials

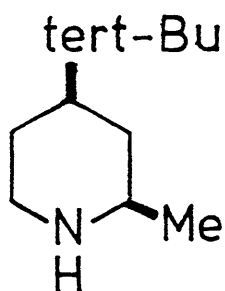
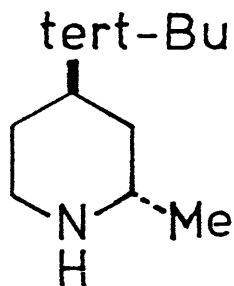
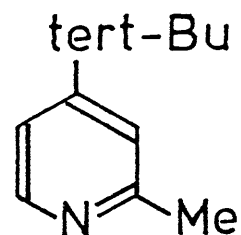
Synthesis of 7 has been described in Chapter 1.<sup>15)</sup> The bipiperidines 8 and 9 were prepared by the silver(I)-catalyzed peroxodisulfate oxidation of the corresponding piperidines [See equation (4.1)]. Preparation of cis-4-tert-butyl-2-methylpiperidine (10) was accomplished by catalytic hydrogenation of 4-tert-butyl-2-methylpyridine (12), which was prepared by methylation of 4-tert-butylpyridine with methyllithium.



7: R=H

8: R=Me

9: R=tert-Bu

101112

#### 4.3 $^{13}\text{C}$ NMR Spectra of cis- (10) and trans-4-tert-butyl-2-methylpiperidines (11)

$^{13}\text{C}$  NMR spectra of 10 and 11, the latter being the by-product in the catalytic hydrogenation of 12, are summarized in Table 4.1 (p.60). Calculated chemical shifts of 10 and 11 were obtained for the 2-methyl equatorial conformation and the 2-methyl axial conformation, respectively, using the parameters of Eliel et al. for methylpiperidines.<sup>16)</sup> Effects of the equatorial tert-butyl group to the chemical shifts of the ring carbon, which was not included in parameters of Eliel et al. or of Booth et al.,<sup>17)</sup> were estimated by comparison of chemical shifts of tert-butylcyclohexane ( $\delta$  48.4(C1), 27.7(C2), 27.3(C3), 26.7(C4))<sup>18)</sup> with the chemical shift of cyclohexane ( $\delta$  26.9)<sup>19)</sup>; the tert-butyl group causes down field shift of 21.5, 0.8, 0.4 and -0.2 ppm at  $\alpha$ ,  $\beta$ ,  $\gamma$  and  $\delta$  positions,

respectively. Thus, for 10,

$$\delta(\text{C2}) = 47.61 + 5.04 + 0.4 = 53.05$$

$$\delta(\text{C3}) = 27.37 + 7.72 + 0.8 = 35.89$$

$$\delta(\text{C4}) = 25.30 - 0.11 + 21.5 = 46.69$$

$$\delta(\text{C5}) = 27.37 - 0.92 + 0.8 = 27.25$$

$$\delta(\text{C6}) = 47.61 - 0.15 + 0.4 = 47.86$$

Chemical shifts of 11 were calculated in a similar fashion.

Agreement of the observed and the calculated chemical shifts is fairly good (within  $\pm 0.8$  ppm). The peaks for C2, C3, C5, 2-Me, and  $-\text{CMe}_3$  in 10 and the peaks for C2, C5, 2-Me, and  $-\text{CMe}_3$  in 11 were assigned from the calculated data, the off-resonance spectra and/or the signal intensities. Assignment of the peaks for C4 and C6 in 10, which overlapped each other, was based on the spin-lattice relaxation times  $T_1$ , which were measured by the inversion recovery method;<sup>20)</sup> the methine carbon C4 ( $T_1$ , 4.2 s) and the methylene carbon C6 ( $T_1$ , 2.4 s) were clearly differentiated. The peaks for C3 and  $-\text{CMe}_3$  in 11 were assigned in a similar manner. Thus, on the basis of the analysis of the  $^{13}\text{C}$  NMR spectra, the configurations and conformations of 10 and 11 were established.

Table 4.1.  $^{13}\text{C}$  NMR Spectra of cis- (10) and trans-4-tert-Butylpiperidines (11) in  $\text{CDCl}_3$

Position	$\delta_{\text{obs}}$	<u>10</u>			$\delta_{\text{obs}}$	<u>11</u>	
		$\delta_{\text{calc}}$	$M^{\text{a)}}$	$T_1/\text{s}$		$\delta_{\text{calc}}$	$M^{\text{a)}}$
2	52.61	53.0	d	4.1	47.46	46.9	d
3	35.86	35.8	t	2.5	32.20	32.9	
4	46.94	46.6		4.2	(40.07) <sup>b)</sup>	40.6	
5	27.11	27.2		2.3	28.11	28.1	
6	47.22	47.8		2.4	(40.20) <sup>b)</sup>	41.0	
<u>2</u> -CH <sub>3</sub>	23.18		q	2.3	17.92		q
- <u>C</u> (CH <sub>3</sub> ) <sub>3</sub>	32.26		s	17.3	32.14		
-C( <u>CH</u> <sub>3</sub> ) <sub>3</sub>	27.34			2.1	27.20		q

a) Multiplicity determined by off-resonance decoupling. b) Assignments may be exchanged.

4.4 Variable Temperature  $^{13}\text{C}$  NMR of 7, 8, and 9

The  $^{13}\text{C}$  NMR spectra of the three bipiperidines at various temperatures are summarized in Table 4.2 (p.62). All of the peaks except for those of the methyl carbons of the tert-butyl groups split into two peaks of equal intensity as the temperature was lowered [See Figures 4.3, 4.4, and 4.5 (p.63, 64, and 65, respectively)]. For 7, below  $-45\text{ }^{\circ}\text{C}$  each of the equally split peaks further splits into two peaks with intensity ratio of ca. 85 : 15 (See Figure 4.3). Arguments for the assignment of the signals will appear in Section 4.7.

The activation parameters for the rate process were calculated by the total line shape analysis (TLS) as well as by the coalescence temperature ( $T_c$ ) method<sup>21</sup>). They are summarized in Table 4.3 (p.66). The agreement between  $\Delta G_c^\ddagger$  values calculated by TLS and those by the  $T_c$  method for a rate process is good. Activation parameters obtained from different peaks in one compound agree well.

Table 4.2.  $^{13}\text{C}$  NMR Data for meso-1,1'-Bi(2-methylpiperidine)s

Compound	<u>7</u>						<u>8</u>				<u>9</u>			
Solvent	THF- $\text{d}_8$ /CS $_2$ =5/6						Diglyme- $\text{d}_{14}$				Diglyme- $\text{d}_{14}$			
Temp/°C	25	-45		-117			146	21			145	48		
Signal	$\delta$ , m <sup>a)</sup>	$\delta$	Ass. <sup>b)</sup>	$\delta$	( $\delta$ ) <sup>c)</sup>	Int. <sup>d)</sup>	$\delta$ , m <sup>a)</sup>	$\delta$ ( $\delta$ ) <sup>c)</sup>	T <sub>1</sub> /s	Ass. <sup>b)</sup>	$\delta$ , m <sup>a)</sup>	$\delta$	T <sub>1</sub> /s	Ass. <sup>b)</sup>
C2,2'	57.95 d	58.53	2'	59.29(59.38) 58.49(57.53) 56.76	w s w		57.51 d	58.23(57.53) 56.17(56.44)	2.0 1.8	2'	58.19 d	58.84 56.71	1.8 1.4	2'
C6,6'	48.74 t	55.20	6	55.93(52.31) 50.93(54.19) 42.11	s w s		e)	56.35(52.31) 42.74(46.78)	1.2 1.2	6	e)	56.78 43.19	1.1 0.9	6
C3,3'	36.45 t	36.34	f)	36.65(36.44) 35.35(36.44) 36.17	s w s		46.38 t	46.01(44.46) 45.60(44.46)	1.2 1.2	f)	38.77 t	38.47 38.14	0.9 0.9	f)
C5,5'	27.63 t	27.89	f)	27.78(28.42) 27.07	s g)		36.36 t	36.36(36.44) 35.48(36.44)	1.0 1.1	f)	28.20	28.91 38.14	1.0 0.9	f)
C4,4'	24.64 t	24.86	f)	26.93(28.42) 25.46(26.62) 24.36	s s f)		31.84 d	31.94(33.34) 31.10(33.34)	2.1 1.9	f)	47.74 d	47.59 46.75	1.7 1.7	f)
2,2'-CH <sub>3</sub>	20.37 q	22.36	2	22.84 19.79 21.17 11.96	s w s w		21.41 q	22.54 20.78	1.0 1.3	2	21.74 q	22.78 20.96	1.1 1.2	2
4,4'-CH <sub>3</sub>							22.00 q	22.36 21.95	1.2 1.1	f)				
4,4'-C(CH <sub>3</sub> ) <sub>3</sub>											32.40 s	32.36 32.18	16.2 i)	f)
4,4'-C(CH <sub>3</sub> ) <sub>3</sub>											27.78 q	27.67	0.9	h)

a) Multiplicity determined by off-resonance decoupling. b) Assignment referred to the Newman projection of Fig. 4.5. c) Calculated chemical shift. See the text. d) Signal intensities are classified into strong(s) and weak(w). Peaks s and w correspond to those for G-SReeee (G+SReeee) and G+SSeeee (G-RReeee), respectively. e) The signal still collapsed into the base line. f) Relative assignments uncertain. g) The signal was not detected. h) The signal did not split. i) T<sub>1</sub> measurements were unsuccessful.



Figure 4.3. Variable temperature  $^{13}\text{C}$  NMR spectra of meso-1,1'-bi(2-methylpiperidine) (7): (i) in diglyme- $\text{d}_{14}$ ; (ii), (iii), and (iv) in  $\text{THF-}d_8/\text{CS}_2 = 5/6$ .

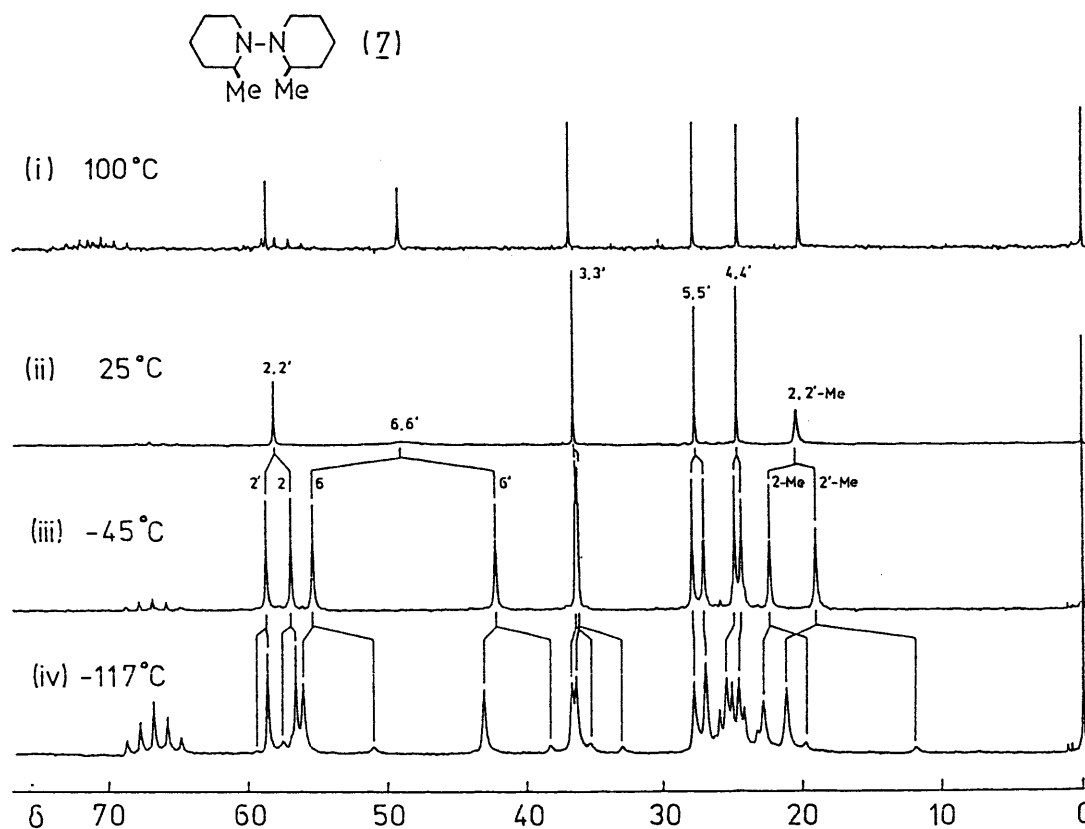


Figure 4.4. Variable temperature  $^{13}\text{C}$  NMR spectra of meso-1,1'-bi(cis-2,4-dimethylpiperidine) (8) in diglyme- $\text{d}_{14}$ .

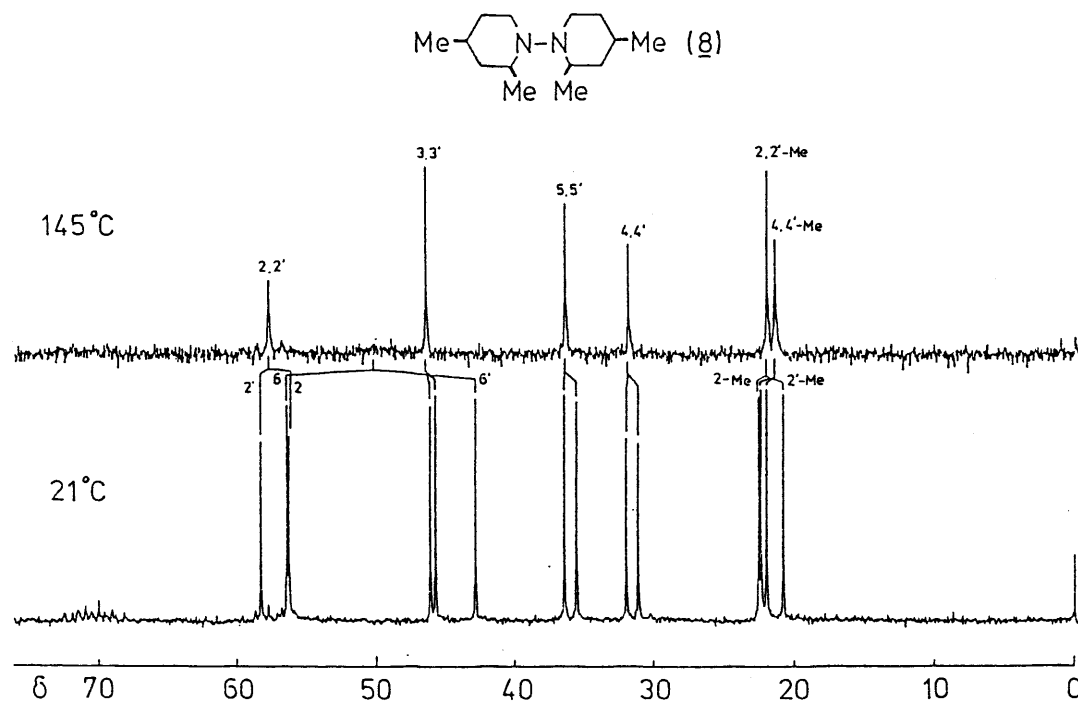


Figure 4.5. Variable temperature  $^{13}\text{C}$  NMR spectra of meso-1,1'-bi(cis-4-tert-butyl-2-methylpiperidine) (9) in diglyme- $d_{14}$ .

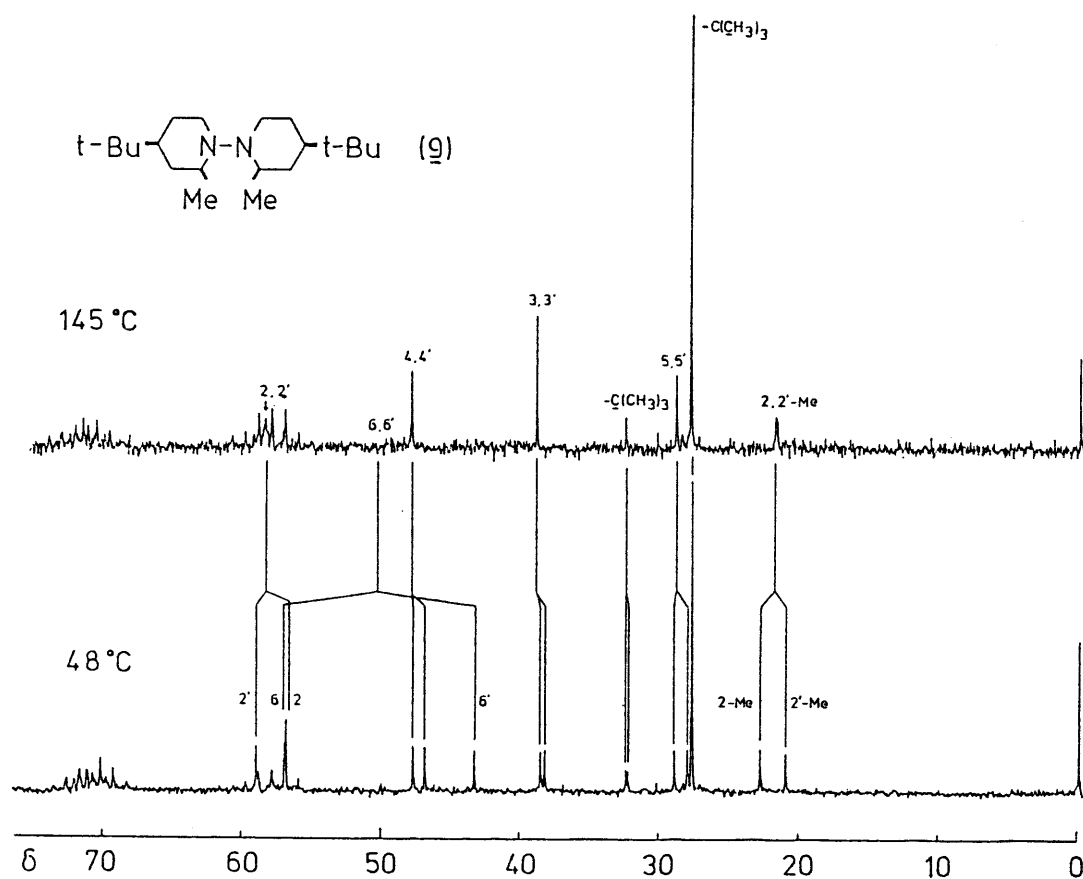


Table 4.3. Activation Parameters for Conformational Process in meso-1,1'-Bi(2-methylpiperidine)s

Compd	Signal	Line Shape Analysis				Coalescence Temp Analysis				Assignment
		Temp range <sup>a)</sup>	$\Delta H^\ddagger$ b)	$\Delta S^\ddagger$ c)	$\Delta G^\ddagger_{298}$ d)	$\Delta\nu/\text{Hz}$	$T_c/^\circ\text{C}$	$\Delta G^\ddagger_c$ d)	$\Delta G^\ddagger_c$ d,e)	
<u>7</u> <sup>f)</sup>	C2,2'	-45 ~ 15	11.86 $\pm$ 0.24	-2.93 $\pm$ 0.96	12.74 $\pm$ 0.05	40.0	-18	12.57 $\pm$ 0.05	12.60 $\pm$ 0.00	G-SReeee $\neq$ G+SReeee
	C3,3'					3.9	-40	12.52 $\pm$ 0.10		
	C5,5'	-45 ~ -1	11.80 $\pm$ 0.43	-3.14 $\pm$ 1.74	12.67 $\pm$ 0.1	18.6	-25	12.60 $\pm$ 0.05	12.52 $\pm$ 0.00	
	C4,4'					11.2	-29	12.62 $\pm$ 0.07		
	2,2'-Me	-41 ~ 25	11.70 $\pm$ 0.22	-3.60 $\pm$ 0.81	12.76 $\pm$ 0.02	75.2	-10	12.64 $\pm$ 0.05	12.64 $\pm$ 0.00	
	2-Me	-106 ~ -55	7.07 $\pm$ 0.56	-9.84 $\pm$ 3.13	9.90 $\pm$ 0.34	210.0	~-82		9.20 $\pm$ 0.00	G-SReeee $\neq$ G+SSeeee and
	C6	-106 ~ -59	6.86 $\pm$ 0.79	-11.28 $\pm$ 4.11	10.23 $\pm$ 0.45	105.5	~-90		8.92 $\pm$ 0.02	G+SReeee $\neq$ G-RRaeae
<u>8</u> <sup>g)</sup>	C3,3'					9.3	62	17.66 $\pm$ 0.07		G-SReeee $\neq$ G+SReeee
	C5,5'	31 ~ 103	17.10 $\pm$ 0.62	-1.77 $\pm$ 1.82	17.64 $\pm$ 0.07	20.5	72	17.69 $\pm$ 0.05	17.71 $\pm$ 0.01	
	C4,4'	31 ~ 103	17.17 $\pm$ 0.67	-1.57 $\pm$ 1.98	1.98 $\pm$ 0.10	19.5	71	17.66 $\pm$ 0.05	17.76 $\pm$ 0.01	
<u>9</u> <sup>g)</sup>	C4,4'	48 ~ 145	17.53 $\pm$ 0.45	-4.03 $\pm$ 1.24	18.74 $\pm$ 0.07	19.0	97	19.07 $\pm$ 0.07	19.03 $\pm$ 0.01	G-SReeee $\neq$ G+SReeee
	C3,3'	48 ~ 95	17.84 $\pm$ 0.67	-3.09 $\pm$ 1.94	18.76 $\pm$ 0.10	7.3	80	18.83 $\pm$ 0.10	18.93 $\pm$ 0.01	
	2,2'-Me	48 ~ 145	17.50 $\pm$ 0.43	-4.11 $\pm$ 1.20	18.74 $\pm$ 0.10	41.0	105	18.90 $\pm$ 0.05	19.05 $\pm$ 0.01	

a)  $^\circ\text{C}$ . b)  $\text{kcal mol}^{-1}$ . c)  $\text{cal K}^{-1}\text{mol}^{-1}$ . d)  $\text{kcal mol}^{-1}$ . e) From Line Shape Analysis. f) In THF- $d_8$ / $\text{CS}_2$ =5/6. g) In diglyme- $d_{14}$ .

## 4.5 Discussion

The Most Stable Conformations of 7, 8, and 9

It is established that in the most stable conformation of 1,1'-bipiperidine the lone pair electrons of the nitrogen atoms are approximately gauche to each other (the torsion angle  $\approx 90^\circ$ ) with the N-N bond equatorial to each of the chair form piperidine rings.<sup>3)</sup> Hence the most stable conformation of the bipiperidines 7, 8, and 9 are certainly the enantiomeric gauche conformations designated as G-SReeee and G+SReeee, in which the N-N bond and all of the alkyl groups are equatorial to each of the piperidine rings, as shown in Figure 4.6 (p.68 - 69). The nomenclature of the conformations will be explained later. When the interconversion between the two conformations is fast on the time scale of NMR, the two piperidine units are equivalent and the bipiperidines have an apparent  $C_2$  symmetry. When the interconversion becomes slow, the apparent  $C_2$  symmetry disappears and the signal splittings with the intensity ratio of 1 : 1 occur. Calculated chemical shifts for G-SReeee (G+SReeee) in 7 and 8 are consistent with the observed chemical shifts (See Section 4.7). Hence, the observed rate processes for 7 over  $-45^\circ\text{C}$  and for 8 and 9 correspond to the interconversion between G-SReeee and G+SReeee.

Figure 4.6. All of the typical gauche and trans conformations in meso-1,1'-bi(2-methylpiperidine) (7), meso-1,1'-bi(cis-2,4-dimethylpiperidine) (8), and meso-1,1'-bi(cis-4-tert-butyl-2-methylpiperidine) (9). Symbol 2-e (2-a) in the Newman projections indicates that the 2-methyl group is equatorial (axial). Symbols 2'-e and 2'-a have analogous meanings for the 2'-methyl group. Symbol e (a) written on a lone pair indicates that the lone pair is equatorial (axial). Heavy lines connecting each of the conformations represent inversions of the piperidine rings.

See the next page.

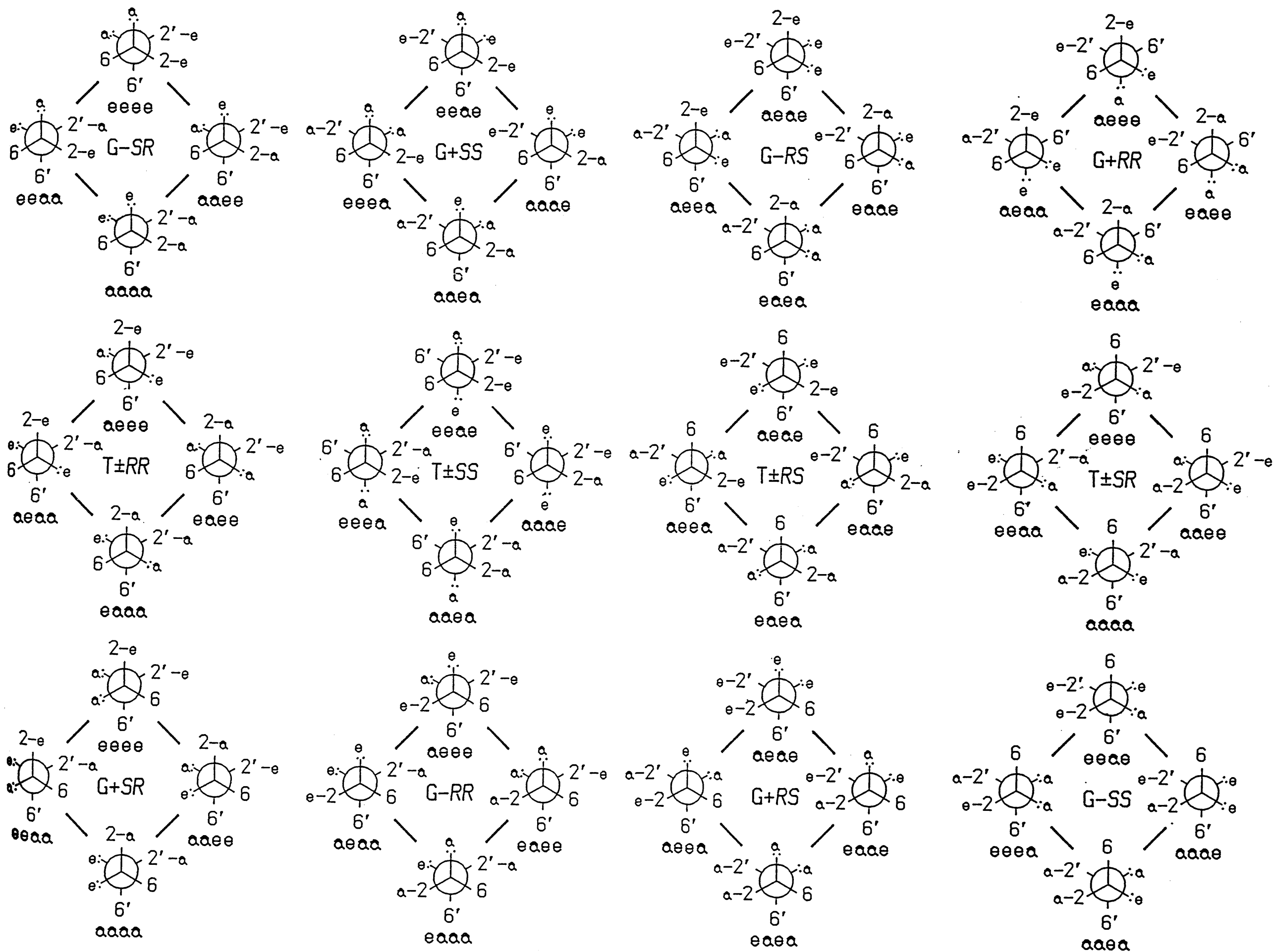
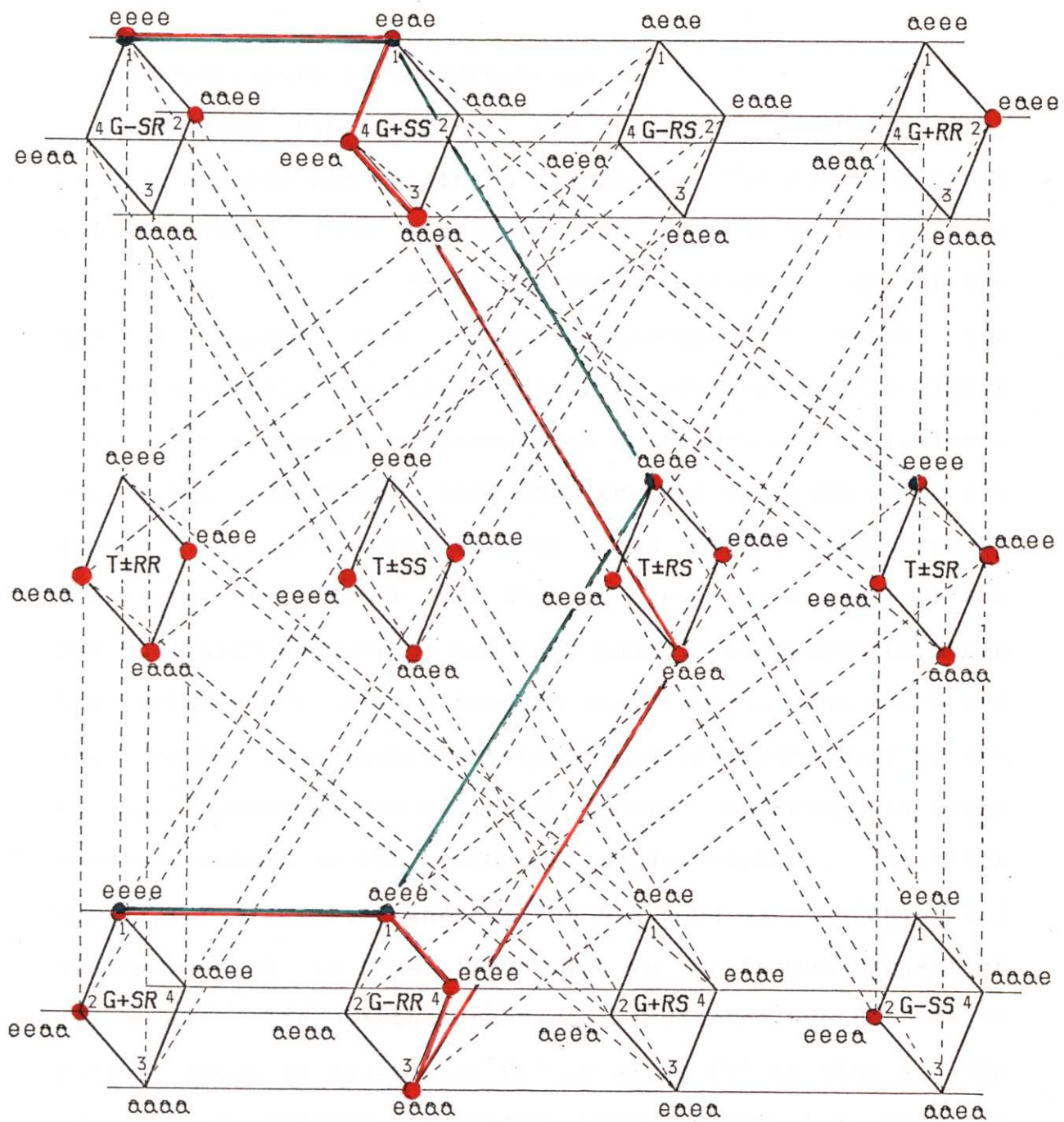


Figure 4.7. Conformational diagram for meso-1,1'-bi(2-methylpiperidine) (7), meso-1,1'-bi(cis-2,4-dimethylpiperidine) (8), and meso-1,1'-bi(cis-4-tert-butyl-2-methylpiperidine) (9). A light, a broken, and a heavy line represent a non-passing nitrogen inversion, a passing nitrogen inversion, and a ring inversion, respectively. Red spots represent the sterically possible conformations in 7 and 8, and red lines represent the lowest barrier one of the inversion paths in these compounds; green spots represent the sterically possible conformation in 9 and green lines represent the lowest barrier one of the inversion path in this compound.

See the next page.





## Nomenclature of Conformations

In the biperidines the nitrogen inversion (the passing and the non-passing N-inversion), the rotation about the N-N bond (the single-passing and the double-passing rotation), and the ring inversion operate. All of the typical gauche and trans conformations which are interconvertible by these processes are depicted in Figure 4.6. We designate conformations in Figure 4.6 as follows. The first descriptor indicates whether the lone pairs are gauche (G) or trans (T) to each other. The second descriptor represents the sign of the torsion angle of the N-N bond with respect to the lone pairs. We designate these two descriptors as the torsion descriptors. The third and the fourth descriptors represent the configurations of the nitrogen atoms N1 and N1', respectively. We designate these two descriptors as the configuration descriptors. The fifth descriptor indicates whether the N-N bond is equatorial (e) or axial (a) to the front ring in the Newman projection (ring A). The sixth descriptor indicates whether the 2-methyl group is equatorial (e) or axial (a) to ring A. The seventh descriptor indicates whether the N-N bond is equatorial (e) or axial (a) to the rear ring in the Newman projection (ring B). The last descriptor indicates whether the 2'-methyl group is equatorial (e) or axial (a) to ring B. We designate the last four descriptors as the ring

conformation descriptors.

#### Conformational Diagram

In the conformational diagram [Figure 4.7 (p.70 - 71)], each of the conformations is placed at corners of the squares. Each of the squares is designated in terms of the torsion and the configuration descriptors. Conformations on each of the squares are interconvertible by ring inversions, for which the torsion and the configuration descriptors are invariant. An inversion of ring A causes changes of the first two of the ring conformation descriptors. An inversion of ring B causes changes of the last two of the ring conformation descriptors.

Horizontal lines connecting corners of the different squares represent non-passing N-inversions. Dotted lines connecting corners of different squares represent passing N-inversions. A non-passing N-inversion causes an interconversion from G to G and a passing N-inversion causes an interconversion from G to T or from T to G. A nitrogen inversion (passing or non-passing) of N1 changes the first one of the ring conformation descriptors and a nitrogen inversion of N1' changes the third one of the ring conformation descriptors.

Rotational processes are not depicted in the diagram to avoid complication. They can be represented by connecting

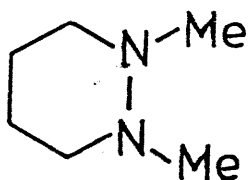
corners having the same configuration and ring conformation descriptors. Thus the corresponding corners of the following squares are connected by single-passing rotations:  $G-SR - T_{+}SR - G+SR$ ,  $G+SS - T_{+}SS - G-SS$ ,  $G-RS - T_{+}RS - G+RS$ , and  $G+RR - T_{+}RR - G-RR$ . Double-passing rotations are given by the following connections:  $G-SR - G+SR$ ,  $G+SS - G-SS$ ,  $G-RS - G+RS$ , and  $G+RR - G-RR$ .

Rotating Newman projections of the gauche conformations in the bottom series by  $180^{\circ}$  with respect to the axis which bisects the N-N bond orthogonally, we can understand that each of the sixteen gauche conformations in the top series has a corresponding enantiomeric gauche conformation in the bottom series. Enantiomeric relationships exist between the same numbered corners of  $G-SR$  and  $G+SR$ , between those of  $G+SS$  and  $G-RR$ , between those of  $G-RS$  and  $G+RS$ , and between those of  $G+RR$  and  $G-SS$ . For example, the enantiomer of  $G-SR_{aaee}$  is  $G+SR_{eeaa}$ .

Our task is to find the lowest barrier path for the interconversion between  $G-SR_{eeeee}$  and  $G+SR_{eeeee}$ . As stated in Section 4.1, the double-passing rotation cannot be involved in the lowest barrier path. Hence, the double-passing rotation is excluded from consideration. As a result, one of the trans conformations must be involved in the interconversion between the two enantiomeric gauche conformations.

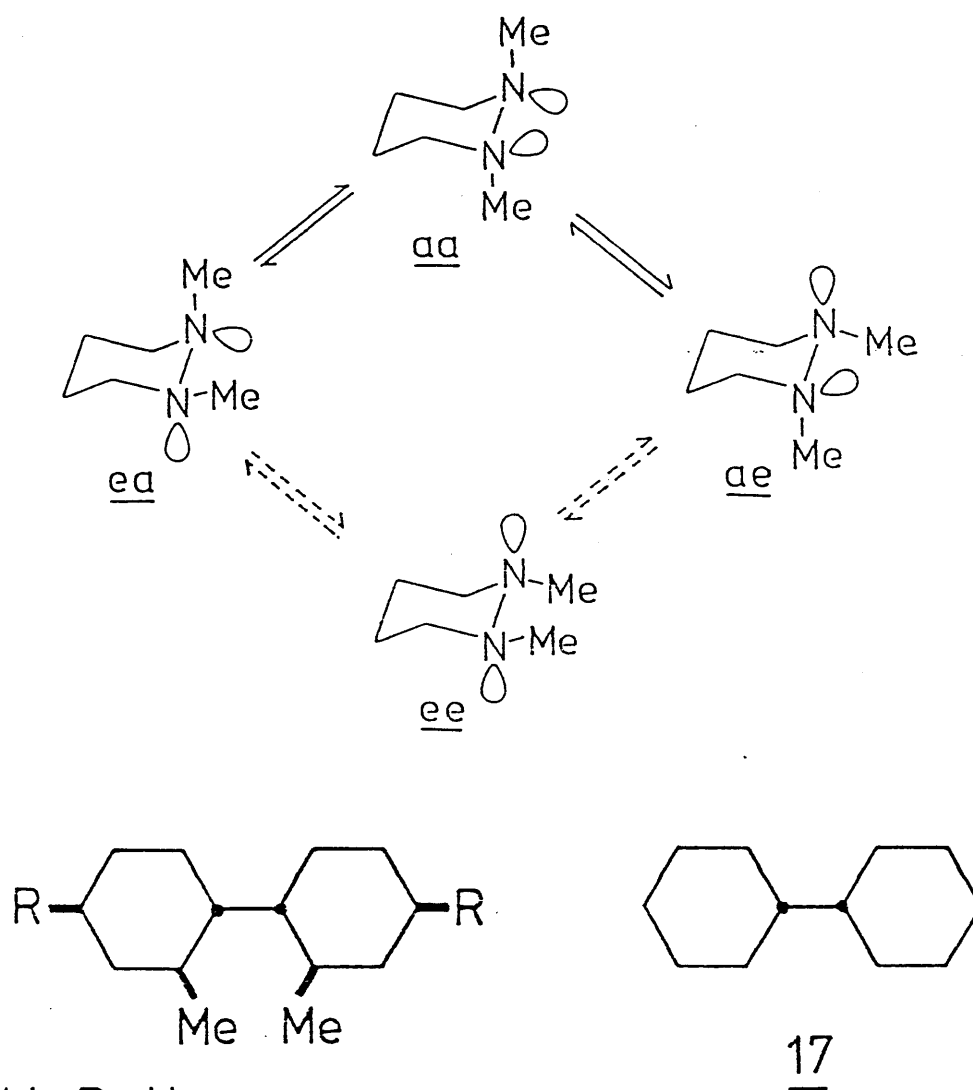
Since in the transition state of a non-passing N-inversion substituents are nearly staggered as shown in Figure 4.1, the barrier to a non-passing N-inversion is likely insensitive to steric factors of the substituents. In contrast, the barrier to a passing N-inversion is likely sensitive to steric factors of substituents, since the substituents are nearly eclipsed in its transition state. As stated in Section 4.1, the principal cause of the barrier difference between the non-passing N-inversion and the passing N-inversion is the electronic interaction. The barrier differences between the passing N-inversions, in which the electronic interaction operates equally, must be ascribed to the steric effects. We designate paths for the interconversion that do not involve a single-passing rotation as inversion paths. There are inversion paths which involve ring inversions. The barrier to ring inversions in cyclohexanes and piperidines seems to be insensitive to substituents on the ring and is in the range of  $10 - 13 \text{ kcal mol}^{-1}$  ( $\Delta G^\ddagger$ ).<sup>22)</sup> This value is substantially smaller than our observed barrier values for 8 and 9. This fact cannot be explained if a ring inversion is the rate determining step in inversion paths. We assume, therefore, that the transition state of an inversion path lies in a passing N-inversion and that the steric interaction in the transition state is similar to that in the trans

conformation involved. This means that the lowest barrier path of inversion paths should involve the trans conformation with the lowest energy. In view of the fact that the interconversion between the most stable conformations ea and ae of 1,2-dimethylperhydropyridazine (13) occurs most easily through the less stable conformer aa rather than the more stable conformer ee [See Figure 4.8 (p.77)],<sup>10)</sup> our assumption might appear to be risky. But in the case of 13 the electronic interaction in the transition state is quite different for the two pathways: While the interconversion through aa is the non-passing N-inversion, that through ee is the passing N-inversion. In contrast, in our case, the electronic interaction is likely approximately equal in all of the inversion paths, since they involve uniformly a passing N-inversion. Therefore, it seems reasonable to assume that the energy of the transition state parallels the steric energy of the trans conformations.



13

Figure 4.8. A partial diagram for the conformational interconversion of 1,2-dimethylperhydropyridazine (13)<sup>10</sup>. A solid and a broken arrow represent a non-passing and a passing N-inversion, respectively.



## Molecular Mechanics Calculations

The potential energy of the bipiperidines is divided into the steric energy and the electronic energy. The steric energy should be similar to that of the corresponding hydrocarbons, which have C-H bonds in place of the nitrogen lone pairs. The electronic energy largely depends upon the torsion angle of the N-N bond. Hence, the relative stability of conformations with the same torsion angle is considered to be parallel with that of the corresponding hydrocarbons.

We have carried out molecular mechanics calculations (MMI)<sup>23)</sup> for the corresponding hydrocarbons 1,1'-bi(2-methylcyclohexane) (14), 1,1'-bi(cis-2,4-dimethylcyclohexane) (15), and 1,1'-bi(cis-4-tert-butyl-2-methylcyclohexane) (16) in all of the conformations depicted in Figure 4.6, since parameters for the N-N bond have not been established. The results are summarized in Table 4.4 (p.79 - 80). Based on these results, we can roughly estimate the relative stability of the conformations in the bipiperidines. Our statement that the most stable conformations in the bipiperidine are the enantiomeric gauche conformations G-SReeee and G+SReeee has been confirmed also by molecular mechanics calculation.



Table 4.4. Molecular Mechanics Calculation of the Corresponding Hydrocarbons for the Bipiperidines

No.	Conformation	Compound <sup>a)</sup>					
		<u>14</u>		<u>15</u>		<u>16</u>	
		Torsion Angle <sup>b)</sup>	Energy <sup>c)</sup>	Torsion Angle <sup>b)</sup>	Energy <sup>c)</sup>	Torsion Angle <sup>b)</sup>	Energy <sup>c)</sup>
1	G-SReeee	-78.0	0.00	-78.3	0.00	-77.5	0.00
2	G-3Raeee	-57.2	3.97	-64.4	7.56	d)	d)
3	G-SRaaaa	d)	d)	d)	d)	d)	d)
4	G-SReeaa	d)	d)	d)	d)	d)	d)
5	G+SSeeea	89.6	1.15	88.0	4.59	d)	d)
6	G+SSaaea	90.8	5.24	88.7	12.52	d)	d)
7	G+SSaaae	d)	d)	d)	d)	d)	d)
8	G+SSeeae	58.3	3.51	58.0	3.43	56.7	3.28
9	G-RSeaea	d)	d)	d)	d)	d)	d)
10	G-RSaeea	d)	d)	d)	d)	d)	d)
11	G-RSaeeae	d)	d)	d)	d)	d)	d)
12	G-RSeaae	d)	d)	d)	d)	d)	d)
13	G+RRaeae	64.1	4.29	57.3	7.57	d)	d)
14	G+RRaeeee	d)	d)	d)	d)	d)	d)
15	G+RRaeaaa	d)	d)	d)	d)	d)	d)
16	G+RRaeaaa	d)	d)	d)	d)	d)	d)
17	T <sub>+</sub> SReeee	-178.4	15.78	-178.5	16.16	-178.5	16.81
18	T <sub>+</sub> SRaeae	-179.3	9.05	-179.2	13.08	d)	d)
19	T <sub>+</sub> SRaaaa	179.9	4.87	179.9	12.04	d)	d)

20	T <sub>+</sub> SR <sub>ee</sub> aa	179.6	8.74	179.6	12.55	d)	d)
21	T <sub>+</sub> RR <sub>ee</sub> ae	-179.0	8.08	-178.8	11.70	d)	d)
22	T <sub>+</sub> RR <sub>ee</sub> aa	180.0	2.62	-179.9	9.56	d)	d)
23	T <sub>+</sub> RR <sub>ae</sub> aa	-179.6	7.43	-179.6	10.92	d)	d)
24	T <sub>+</sub> RR <sub>ae</sub> ee	d)	d)	d)	d)	d)	d)
25	T <sub>+</sub> RS <sub>ee</sub> ae	180.0	1.02	180.0	7.94	d)	d)
26	T <sub>+</sub> RS <sub>ae</sub> ee	-179.6	5.89	-180.0	8.94	d)	d)
27	T <sub>+</sub> RS <sub>ae</sub> ae	180.0	11.05	180.0	10.88	180.0	10.16
28	T <sub>+</sub> RS <sub>ee</sub> ae	179.9	5.58	180.0	8.94	d)	d)
29	T <sub>+</sub> SS <sub>ee</sub> ee	179.1	7.51	179.0	11.09	d)	d)
30	T <sub>+</sub> SS <sub>ae</sub> ae	-180.0	2.64	179.9	9.56	d)	d)
31	T <sub>+</sub> SS <sub>ae</sub> ae	179.6	7.43	179.6	10.94	d)	d)
32	T <sub>+</sub> SS <sub>ee</sub> ae	d)	d)	d)	d)	d)	d)

---

a) The hydrocarbons 14, 15, and 16 correspond to the bipieridines 7, 8, and 9, respectively (See the text).  
b) Torsion angle  $\omega$  with respect to the H - C1 - C1' - H in degree. c) Final steric energy in kcal mol<sup>-1</sup>.  
The energies of the most stable conformation G-SR<sub>ee</sub>ee in each compound (23.48, 23.86, and 36.70 kcal mol<sup>-1</sup> for 14, 15, and 16, respectively) were set to 0.00 kcal mol<sup>-1</sup>. d) Sterically impossible conformation.

## The Lowest Barrier Inversion Path

The most stable one of the trans conformations in 7 is  $T_+RSeaea$ . Gauche conformations which can directly arrive at  $T_+RSeaea$  by a passing N-inversion are formally  $G+SSaaea$ ,  $G-RReaaa$ ,  $G+RReaaa$ , and  $G-SSaaea$ . The last two conformations,  $G+RReaaa$  and  $G-SSaaea$ , are sterically impossible conformations. The sterically possible gauche conformation which can directly arrive at  $G+SSaaea$  ( $G-RReaaa$ ) is  $G+SSeeaa$  ( $G-RReaee$ ), which is the next stable gauche conformation. The sterically possible gauche conformation which can arrive at  $G+SSeeaa$  ( $G-RReaee$ ) is  $G+SSeeae$  ( $G-RRaeae$ ), which is accessible only from the most stable conformation  $G-SReeee$  ( $G+SReeee$ ). Therefore the lowest barrier inversion path is the following:  $G-SReeee \rightleftharpoons G+SSeeae \rightleftharpoons G+SSeeaa \rightleftharpoons G+SSaaea \rightleftharpoons T_+RSeaea \rightleftharpoons G-RReaaa \rightleftharpoons G-RReaee \rightleftharpoons G-RRaeae \rightleftharpoons G+SReeee$ .

The lowest barrier inversion path in 8 is the same inversion path as in 7:  $G-SReeee \rightleftharpoons G+SSeeae \rightleftharpoons G+SSeeaa \rightleftharpoons G+SSaaea \rightleftharpoons T_+RSeaea \rightleftharpoons G-RReaaa \rightleftharpoons G-RReaee \rightleftharpoons G-RRaeae \rightleftharpoons G+SReeee$ .

Among the conformations which are sterically possible for 7 or 8, those with an axial methyl group are sterically prohibited in the case of 9 since in these conformations the tert-butyl group must take the axial position which is impossible owing to the 1,3-diaxial interaction with the methyl group. As a result, for 9, there are only two

sterically possible trans conformations,  $T_+RSaeae$  and  $T_+SReeee$ , the former being more stable. Sterically possible gauche conformations which can arrive at  $T_+RSaeae$  are  $G+SSeeae$  and  $G-RRaeae$ .  $G+SSeeae$  ( $G-RRaeae$ ) is accessible only from the most stable conformation  $G-SReeee$  ( $G+SReeee$ ). Hence the lowest barrier inversion path should be the following:  $G-SReeee \rightleftharpoons G+SSeeae \rightleftharpoons T_+RSaeae \rightleftharpoons G-RRaeae \rightleftharpoons G+SReeee$ .

#### The Lowest Barrier Rotation Path

We designate a single-passing rotation path  $G-SReeee \rightleftharpoons T_+SReeee \rightleftharpoons G+SReeee$ , in which neither nitrogen inversion nor ring inversion is involved, as the pure single-passing rotation path. Energy profiles of the pure single-passing rotation path calculated by MMI for 14, 15, 16, and bi(cyclohexane) (17) are shown in Figure 4.9 (p.85 - 86).<sup>24)</sup> The important features of the energy profiles are that except in the case of 17 a staggered conformation  $T_+SReeee$  lies in the saddle point (15.78 - 16.81 kcal mol<sup>-1</sup>) and that it is ca. 6 - 8 kcal mol<sup>-1</sup> higher than other saddle points (8.35 - 10.04 kcal mol<sup>-1</sup>), which correspond to the nearly eclipsed conformations. In Figure 4.9 the energy of the most stable staggered conformation is taken as the reference. It is known that MMI gives reliable steric energies for staggered conformations of hydrocarbons while

it gives lower energies (ca. 10 - 20 % lower) for eclipsed conformations than true values.<sup>25)</sup> Based on this fact, the steric energies of  $T_{+}SR_{eeee}$  are expected to be accurate while the steric energies of the nearly eclipsed conformations can be as large as 10.02 - 12.05 kcal mol<sup>-1</sup>, which are still lower than  $T_{+}SR_{eeee}$ . Hence the transition state of the pure single-passing rotation path is certainly  $T_{+}SR_{eeee}$ . The energies of  $T_{+}SR_{eeee}$ , i.e., the calculated rotational barriers ( $\Delta H^{\ddagger}$ ) for 14, 15, and 16, are 15.78, 16.16, and 16.81 kcal mol<sup>-1</sup>, respectively. The experimental rotational barriers for 14, 15, and 16 are not known. Theoretical calculations of hydrazine have shown that the trans conformation is a saddle point in the N-N bond rotation owing to the electronic interaction.<sup>13)</sup> Hence, in the bipiperidines, both the steric and the electronic effects operate to make  $T_{+}SR_{eeee}$  a saddle point. The barriers for the pure single-passing rotation path in the bipiperidines are expected to be higher than the calculated rotational barrier for 14, 15, and 16, since the N-N bond is shorter than the C-C bond and since in the bipiperidines there would be repulsive interactions between lone pair electrons which do not exist in the hydrocarbons. Although in our first intuition the rotational barrier in 14, 15, and 16 are the same, the calculated barriers increase in the order 14, 15, 16. This increase in the calculated

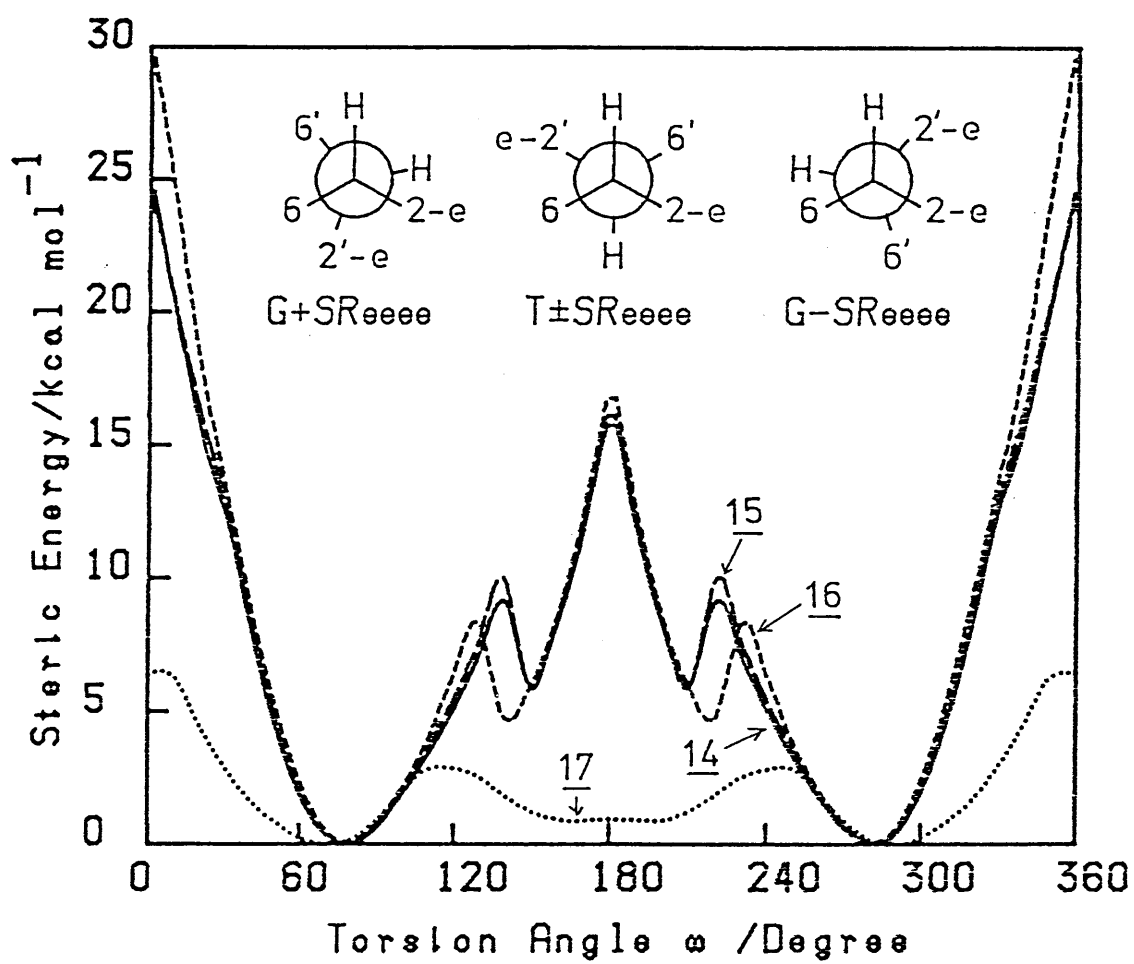
rotational barrier can be ascribed to the increase in the rigidity of the molecules.

We designate paths for the interconversion in which non-passing N-inversion and/or ring inversion are involved in addition to a single-passing rotation as inversion-rotation paths. Since there are impossible gauche and trans conformations, 7 and 8 have only one inversion-rotation path  $G-SReeee \rightleftharpoons G-SRaeee \rightleftharpoons G+RReaee \rightleftharpoons T+RReaee \rightleftharpoons G-RReaee \rightleftharpoons G-RRaeee \rightleftharpoons G+SReeee$ . The inversion-rotation paths of 7 and 8 are, however, impossible because of the severe steric congestion at the eclipsed form (the torsion angle  $\simeq 120^\circ$ ) between  $G+RReaee$  and  $T+RReaee$  in the single-passing rotation, which is easily noticed by the inspection of models. For 9, there is no inversion-rotation path.

Hence, the pure single-passing rotation path is the lowest barrier rotation paths.

Figure 4.9. Energy profiles of the bond rotation about the C1-C1' bond in meso-1,1'-bi(2-methylcyclohexane)(14)(——), meso-1,1'-bi(cis-2,4-dimethylcyclohexane) (15)(— — —), meso-1,1'-bi(cis-4-tert-butyl-2-methylcyclohexane)(16)(- - - - -), and bi(cyclohexane) (17)(.....), calculated by MMI as a function of the torsion angle  $\omega$ (H - C1 - C1' - H). All other internal coordinates are optimized. For 14, 15, and 16, the steric energy of the most stable conformations G-SReeee and G+SReeee in each of the compounds is set to 0.00 kcal mol<sup>-1</sup> (See note c in Table 4.4). For 17 the minimum of the steric energy (18.31 kcal mol<sup>-1</sup> at  $\omega$  = 70.0 and 290.0° ) is set to 0.00 kcal mol<sup>-1</sup>.

See the next page.





### The Inversion Path vs. the Pure Single-Passing Rotation Path

The above discussion has shown that the lowest barrier path for the interconversion between G-SReeee and G+SReeee in each of the bipiperidines is one of the two paths, the inversion path or the pure single-passing rotation path. In Table 4.5 (p.89) the observed barriers of the bipiperidines are compared with the calculated steric energies of the trans conformations involved in the inversion paths and the calculated rotational barriers in the corresponding hydrocarbons. Since the observed barrier for 7 ( $\Delta H^\ddagger = 11.8$  kcal mol<sup>-1</sup>) is substantially lower than the calculated barrier to the single-passing rotation path for 14 ( $\Delta H^\ddagger = 15.78$  kcal mol<sup>-1</sup>), the lowest barrier path in 7 is not the rotation path but the inversion path G-SReeee  $\rightleftharpoons$  G+SSeeae  $\rightleftharpoons$  G+SSeeea  $\rightleftharpoons$  G+SSaaea  $\rightleftharpoons$  T+RSeaea  $\rightleftharpoons$  G-RRaaaa  $\rightleftharpoons$  G-RRaeae  $\rightleftharpoons$  G-RRaeae  $\rightleftharpoons$  G+SReeee. Hence the observed barrier is assigned to the passing N-inversion between G+SSaaea and T+RSeaea and between G-RRaaaa and T+RSeaea.

The difference between the observed barriers of 8 and 9 is much closer to the difference between the calculated rotational barriers of the corresponding hydrocarbons, 15 and 16 than to the calculated energy difference between T+RSeaea of 15 and T+RSaeae of 16. Moreover, the observed barriers of 8 and 9 are slightly higher than the calculated

rotational barriers of 15 and 16. Therefore, we assign the observed barriers of 8 and 9 to the pure single-passing rotation path  $G-S_{Reeee} \rightleftharpoons T-S_{Reeee} \rightleftharpoons G+S_{Reeee}$ . These barriers can be explained by the steric compression which involves a 1,3-diaxial like interaction between the 2-methyl (2'-methyl) group and the equatorial C6'-H (C6-H) across the N1-N1' bond. In fact, the energy profile of 17, which does not have such a steric compression in the trans conformation, shows a minimum with  $0.96 \text{ kcal mol}^{-1}$  at  $\omega = 180.0^\circ$  and saddle points with  $2.85 \text{ kcal mol}^{-1}$  at  $\omega = 120.0^\circ$  and  $240.0^\circ$  (See Figure 4.9).<sup>24)</sup> The observed barrier for 8 and 9 are well compared with the rotatinal barrier ( $\Delta G^\ddagger = 17.4 \text{ kcal mol}^{-1}$  at  $-35^\circ \text{C}$ ) of 2,2'-dimethylbiphenyl.<sup>26)</sup>

Table 4.5. Comparison of the Observed Barriers of the Bipiperidines ( $\Delta H_{\text{obs}}^{\ddagger}$ ) with the Calculated Rotational Barriers ( $\Delta H_{\text{calc}}^{\ddagger}$ ) and the Calculated Steric Energies (SE) of the Trans Conformations Involved in the Inversion Paths in the Corresponding Hydrocarbons.

Bipiperidines		Hydrocarbons		
Compound	$\Delta H_{\text{obs}}^{\ddagger}$ <sup>a,b)</sup>	Compound	$\Delta H_{\text{calc}}^{\ddagger}$ <sup>a,c)</sup>	SE <sup>a,d)</sup>
<u>7</u>	11.80	<u>14</u>	15.78	1.02 (T <sub>+</sub> RS <sub>e</sub> a <sub>e</sub> a)
<u>8</u>	17.14	<u>15</u>	16.16	7.94 (T <sub>+</sub> RS <sub>e</sub> a <sub>e</sub> a)
<u>9</u>	17.63	<u>16</u>	16.81	10.16 (T <sub>+</sub> RS <sub>a</sub> e <sub>a</sub> e)

a) kcal mol<sup>-1</sup>. b) From Table 4.3. c) From Figure 4.9. d) From Table 4.4.

The Lower Temperature Process in 7

The above discussion is further supported by the observation of the lower temperature process in 7. At lower temperatures all of the peaks of 7 further split into two peaks with intensity ratio of about 85 : 15. At  $-117^{\circ}\text{C}$  one of the methyl signals splits to a large extent ( $\Delta\nu = 209.5$  Hz) with the weaker peak appearing at higher field ( $\delta 11.9$ ). The weak peak was unequivocally assigned to the axial methyl group from its  $\delta$  value<sup>27)</sup> (See Table 4.2 and Figure 4.3). These results strongly suggest that at the lower temperature the interconversions between G-SReeee and G+SSeeea via G+SSeeae and between G+SReeee and G-RReaee via G-RRaeae are frozen out. From the ratio of the integrated intensities of the axial and the equatorial methyl signal, the free energy of G+SSeeea (as well as G-RReaee) was estimated to be higher by  $0.55 \text{ kcal mol}^{-1}$  at  $-117^{\circ}\text{C}$  than that of G-SReeee (as well as G+SReeee). The calculated enthalpy difference between G+SSeeea (G-RReaee) and G-SReeee (G+SReeee) in 14 is  $1.15 \text{ kcal mol}^{-1}$  as shown in Table 4.4. The entropy contribution due to symmetry of G+SSeeea (G-RReaee) is zero while that of G-SReeee (G+SReeee) is  $-R\ln 2$  ( $1.38 \text{ cal/deg.mol}$ ), where  $R$  is gas constant. Hence, the calculated free energy difference in 14 between G+SSeeea (G-RReaee) and G-SReeee (G+SReeee) is  $0.94 \text{ kcal mol}^{-1}$  at  $-117^{\circ}\text{C}$ , which is close to the observed experimental free energy

difference in 7.

In view of the fact that the barriers to the non-passing N-inversion ( $\Delta G^\ddagger = 7 - 8 \text{ kcal mol}^{-1}$ ) in 1, 2, and 3 are lower than the barriers to the ring inversion in piperidines ( $\Delta G^\ddagger = 10 - 13 \text{ kcal mol}^{-1}$ ), it is concluded that the transition state corresponding to the observed barrier ( $\Delta G^\ddagger = 9.2 \text{ kcal mol}^{-1}$  at  $-117^\circ\text{C}$ ) to the interconversions of 7 between G-SReeee and G+SSeeea and between G+SRReeee and G-RRaeae lies in the ring inversion processes between G+SSeeae and G+SSeeea and between G-RRaeae and G-RRReae, not in the non-passing N-inversion processes between G-SReeee and G+SSeeae and between G+SRReeee and G-RRaeae. In other words, it is concluded that the observed barrier is the free energy difference between the transition state of the ring inversion processes and the most stable conformations G-SReeee and G+SRReeee. In 8 and 9 the energy difference between the next most stable conformation G+SSeeae (G-RRaeae) and the most stable conformation G-SReeee (G+SRReeee) is so large that the next most stable conformation was not detected irrespective of the slowing down of the conformational interconversion at lower temperature.

#### 4.6 Experimental

VPC was carried out on a Varian-Aerograph Model 920 instrument with a 20 % TRITON X-305 column (1/4 in. 4 m, on 60 - 80 mesh Uniport B. Fractional distillation was carried out on a PERKIN-ELMER NFT-51 spinning band annular still.

#### Materials

cis-2,4-Dimethylpiperidine (18).<sup>28)</sup>

The method of Booth and Little was used for reduction of 3,5-dimethylpyridine.<sup>29)</sup> 2,4-Dimethylpyridine (50 g) was dissolved in hot dry EtOH (800 mL) and Na (85 g) was added with magnetic stirring in small pieces at a rate sufficient to maintain boiling. The mixture was cooled, acidified with hydrochloric acid (30 %) and heated to remove EtOH under reduced pressure. The residue was basified with aq NaOH (40 %) and the liberated base was extracted with ether. Distillation gave a colorless oil (45 g), bp 60 - 67 °C / 52 - 55 mmHg, shown by VPC to contain 58 % of cis-2,4-dimethylpiperidine (18), 10 % of the trans-isomer, 7 % of 1,2,3,6-tetrahydro-2,4-dimethylpyridine, and 24 % of 1,2,5,6-tetrahydro-2,4-dimethylpyridine. The mixture (51.5 g), dissolved in dil. HCl (9 %, 253 mL), was hydrogenated over Adams platinum oxide catalyst (500 mg) until uptake of hydrogen ceased and the catalyst was filtered off. This

procedure was repeated several times and the filtrate was gathered. The usual method of recovery gave a mixture (130 g) of cis-(77 %) and trans- (23 %) 2,4-dimethylpiperidines from 175 g of 2,4-dimethylpyridine. Fractional distillation (reflux ratio 100, bp 140 °C) gave pure 18 (67 g). Its  $^1\text{H}$  NMR spectrum was identical with that reported by Wendisch et al.<sup>30)</sup>  $^{13}\text{C}$  NMR ( $\text{CDCl}_3$ )  $\delta$  52.14 (d; C2), 46.96 (t; C6), 43.78 (t; C3) 35.02 (t; C5), 31.55 (d; C4), 23.10 (q; 2-Me), 22.60 (q; 4-Me).

meso-1,1'-Bi(cis-2,4-dimethylpiperidine) (8).

A 25 % aq solution of sodium peroxodisulfate (35.7 g, 150 mmol) was added dropwise at 0 °C to a stirred mixture of 18 (11.3 g, 100 mmol), sodium hydroxide (12.0 g, 300 mmol) and a catalytic amount of silver nitrate (850 mg, 5 mmol) in water (120 mL) and the mixture was stirred for additional 3.5 h. After the saturation of the reaction mixture with sodium chloride, it was extracted with ether. The ethereal extract was dried over  $\text{Na}_2\text{SO}_4$  and concentrated under reduced pressure. The residue was chromatographed three times on an alumina column using hexane as an eluant to give dl-1,1'-bi(cis-2,4-dimethylpiperidine)(19) (291 mg, yield 2.6 %) and meso-1,1'-bi(cis-2,4-dimethylpiperidine)(8) (140 mg, yield 1.2 %), both of which were colorless oils.  $^{13}\text{C}$  NMR ( $\text{THF}-d_8/\text{CS}_2 = 5/6$ ) of 19  $\delta$  53.70 (d; C2, C2'), 44.19 (t; C6, C6'),

43.26 (t; C3,C3'), 35.22 (t; C5,C5'), 31.77 (d; C4,C4'), 22.39 (q; CH<sub>3</sub>), 22.19 (q; CH<sub>3</sub>). Mass spectrum, m/e 224(M<sup>+</sup>).

Anal for the diastereomeric mixture; Calcd for C<sub>14</sub>H<sub>28</sub>N<sub>2</sub>: C, 74.94; H, 12.58; N, 12.49. Found: C, 75.20; H, 12.46; N, 12.34.

#### 4-tert-Butyl-2-methylpyridine (12).

The method of Ziegler and Zeiser was used for methylation of pyridines.<sup>31)</sup> To a stirred solution of methyllithium, prepared from methyl iodide (142 g, 1 mol) and lithium ribbon (17 g, 2.4 mol) in ether,<sup>32)</sup> 4-tert-butylpyridine was added dropwise for 3.5 h. After 550 mL of dry toluene was added, ether was distilled off, and the solution was refluxed for 14 h. The solution was cooled with ice bath. The generated lithium hydride and the unchanged methyllithium were decomposed by adding ice into the solution. The solution was acidified with hydrochloric acid (6N), and the separated water layer was basified with aq NaOH (40 %). The liberated base was extracted with ether and the extract was dried over Na<sub>2</sub>SO<sub>4</sub> and KOH. Distillation gave a colorless oil (102 g)(bp 101 - 106 °C / 40 mmHg), which was shown by VPC, as well as NMR, to contain 63 % of 4-tert-butyl-2-methylpyridine (12) and 37 % of unchanged 4-tert-butylpyridine. Fractional distillation gave a mixture (40 g) of 12 (90 %) and 4-tert-butylpyridine (10%), which



was used in the catalytic hydrogenation. Preparative VPC and the subsequent distillation gave a colorless oil as an analytically pure sample of 12.  $^1\text{H}$  NMR ( $\text{CDCl}_3$ )  $\delta$  8.38 (1H, d,  $J = 5$  Hz), 7.2 - 6.8 (2H, m), 2.55 (3H, s), 1.30 (9H, s); mass spectrum,  $m/e$  149( $\text{M}^+$ ).

Anal. Calcd for  $\text{C}_{10}\text{H}_{15}\text{N}$ : C, 80.48; H, 10.13; N, 9.39. Found: C, 80.53; H, 10.18; N, 9.32.

cis-4-tert-Butyl-2-methylpiperidine (10).

Raney nickel-aluminium alloy (40 %, 4 g) was added slowly to a stirred aq solution of sodium hydroxide (20 %, 100 mL), which was heated at ca. 50 °C, and it was stirred for an additional 15 min at the same temperature. The supernatant layer was removed by decantation and the nickel residue was washed with water. To the residue, tert-butyl alcohol (50 mL) and 12 (40 g, contained 10 % of 4-tert-butylpyridine) were added and the mixture was heated at 60 - 70 °C for 1 h with stirring. The catalyst was filtered off and the filtrate was placed in an autoclave. To the solution,  $\text{Ru}(\text{OH})_3$  (600 mg)<sup>33)</sup> and  $\text{LiOH}\cdot\text{H}_2\text{O}$  (100 mg) were added and the mixture was hydrogenated at 40 atm, 80 - 120 °C. Hydrogen absorption continued for 5 h. THF (50 mL) was added to the mixture and the solution was filtered through a double layer of  $\text{MgSO}_4$  and cellulose powder. The filtrate was acidified with hydrochloric acid (10 %) and evaporated.

The residue was basified with aq solution of NaOH (20 %) and was extracted with ether. The extract was dried over  $\text{MgSO}_4$ , concentrated under reduced pressure, and dried again over KOH. Distillation gave 32 g of a colorless oil (bp 92 - 94 °C / 28 - 30 mmHg), which was shown by VPC, as well as NMR, to contain 85 % of cis-4-tert-butyl-2-methylpiperidine (10), 6 % of trans-4-tert-butyl-2-methylpiperidine (11) and 9 % of 4-tert-butylpiperidine. The distillate was used as the material for the N-N coupling reaction. Preparative VPC gave 10 as a colorless oil and 11 as an easily sublimable, colorless solid (mp 59.0 - 60.0 °C).

10:  $^1\text{H}$  NMR ( $\text{CDCl}_3$ )  $\delta$  3.25 - 3.00 (1H, m), 2.75 - 2.35 (2H, m), 1.80 - 1.45 (3H, m), 1.4 - 0.7 (3H, m), 1.07 (3H, d,  $J = 6$  Hz), 0.88 (9H, s); IR (neat)  $3250\text{ cm}^{-1}$  (N-H); mass spectrum,  $m/e$  155 ( $\text{M}^+$ ).

Anal. Calcd for  $\text{C}_{10}\text{H}_{21}\text{N}$  : C, 77.35; H, 13.63; N, 9.02. Found: C, 77.22; H, 13.59; N, 8.87.

11: Mass spectrum (high resolution),  $m/e$  155.1679 (155.1674 calcd for  $\text{C}_{10}\text{H}_{21}\text{N}$ );  $^1\text{H}$  NMR ( $\text{CDCl}_3$ )  $\delta$  3.58 - 3.18 (1H, br.s), 2.95 - 2.72 (2H, m), 2.70 (1H, s), 1.75 - 1.05 (5H, m), 1.18 (3H, d,  $J = 7$  Hz), 0.85 (9H, s); IR (nujol)  $3410\text{ cm}^{-1}$  (N-H).

meso-1,1'-Bi(cis-4-tert-butyl-2-methylpiperidine)(9).

A 25 % aq solution of sodium peroxodisulfate (25.0 g,

105 mmol) was added dropwise below 10 °C to a stirred mixture of 10 (a mixture of 85 % of 10 and 15 % of the trans isomer 11, 10.8 g, 60 mmol), sodium hydroxide (8.4 g, 210 mmol) and a catalytic amount of silver nitrate (595 mg, 3.5 mmol) in water (84 mL) and the mixture was stirred for an additional 4.5 h. After the reaction mixture was saturated with sodium chloride, it was extracted with ether. The extract was dried over Na<sub>2</sub>SO<sub>4</sub> and evaporated under reduced pressure. The residue was chromatographed several times on an alumina column using hexane as an eluant to give dl-1,1'-bi(cis-4-tert-butyl-2-methylpiperidine)(20) (89 mg, yield 1 %), and the meso isomer (9) (40 mg, yield 0.4 %).

20: mp 121.0 - 122.0 °C (needles from MeOH); <sup>13</sup>C NMR (THF-d<sub>8</sub>) δ 54.81 (d, C2, C2'), 47.68 (t, C4, C4'), 44.04 (t; C6, C6'), 37.21 (t; C3, C3'), 32.49 (s; -C(CH<sub>3</sub>)<sub>3</sub>), 28.19 (d; C5, C5'), 27.74 (q; -C(CH<sub>3</sub>)), 21.45 (q; 2-CH<sub>3</sub>, 2'-CH<sub>3</sub>); mass spectrum, m/e 308 (M<sup>+</sup>).

Anal. Calcd for C<sub>20</sub>H<sub>40</sub>N<sub>2</sub> : C, 77.85; H, 13.07; N, 9.08. Found: C, 77.66; H, 12.89; N, 9.07.

9: mp 94.0 - 95.0 °C (prisms from MeOH); mass spectrum, m/e 308 (M<sup>+</sup>).

Anal. Calcd for C<sub>20</sub>H<sub>40</sub>N<sub>2</sub> : C, 77.85; H, 13.07; N, 9.08. Found: C, 77.80; H, 12.79; N, 8.97 %.

$^{13}\text{C}$  NMR Measurements

All of the variable-temperature  $^{13}\text{C}$  NMR spectra were recorded at 22.5 MHz on a JEOL FX90Q spectrometer fitted with a variable temperature controller JEOL NM-VTS. Typical spectrometer settings are as follows: spectral width, 2000 Hz; number of data points, 8 K; pulse angle,  $55^\circ$ . The spectrometer was locked on a deuterium signal from THF- $\text{d}_8$  or diglyme- $\text{d}_{14}$ . All NMR samples were freeze-thaw degassed and sealed in 10 mm o.d. sample tubes. Temperatures were calibrated with a chromel-alumel thermocouple which was inserted, at receiver coil height, into another 10 mm od sample tube containing an equal volume of silicone oil. The accuracy of the quoted temperatures is within  $\pm 1^\circ\text{C}$ .

Line shape calculations were performed on the University of Tokyo HITAC M200H computer using the programs, DNMR3<sup>34)</sup> and LSQM2. The spin-spin relaxation time ( $T_2$ ) was replaced by an effective  $T_2$ , which was estimated from the average of the half-height line width of TMS peak in the whole region of the exchange process. Errors in the enthalpy and entropy of activation are 95 % confidence limits from a least-square fit of the Eyring rate equation. Errors in the free energy of activation was evaluated from the error of enthalpy and entropy of activation by using the equation of Binsch and Kessler.<sup>35)</sup>

In the  $T_c$  method, we obtained the free energy of

activation at the coalescence temperature from the following equation<sup>21)</sup>:

$$\Delta G_c^\ddagger = RT_c \left[ \ln \left( \frac{\sqrt{2R}}{\pi N h} \right) + \ln \left( \frac{T_c}{\Delta \nu} \right) \right] \quad (4.2)$$

where  $R$  is gas const;  $T_c$ , coalescence temperature;  $N$ , Avogadro const;  $h$ , Planck const. Errors in  $\Delta G_c^\ddagger$  ( $\sigma_G$ ) were calculated by applying the well known equation for the propagation of errors<sup>36)</sup> to equation (4.2):

$$\begin{aligned} \sigma_G &= \sqrt{\left( \frac{\partial (\Delta G_c^\ddagger)}{\partial T_c} \right)^2 \sigma_T^2 + \left( \frac{\partial (\Delta G_c^\ddagger)}{\partial (\Delta \nu)} \right)^2 \sigma_{\Delta \nu}^2} \\ &= 8.3144 \sqrt{[23.96 + \ln \left( \frac{T_c}{\Delta \nu} \right)]^2 \sigma_T^2 + \left( \frac{T_c}{\Delta \nu} \right)^2 \sigma_{\Delta \nu}^2} \quad \text{in J mol}^{-1} \end{aligned}$$

where  $\sigma_T$  is the mean error of  $T_c$  in K;  $\sigma_{\Delta \nu}$ , the mean error of  $\Delta \nu$  in Hz.

The  $\Delta G$  difference between G-SReeee and G+SSeeee (or G+SReeee  $\rightleftharpoons$  G-RReeee) in 7 was determined from the equilibrium constant, which was estimated from the peak area ratio of the split peaks of C6'. It was obtained by cutting and weighing the the appropriate portion of the recorded spectra.

4.7 Assignment of  $^{13}\text{C}$  NMR Signals of 7, 8, and 9

Assignment of the signals in the high temperature spectra of 7, 8, and 9 was made on the basis of the off-resonance spectra and of the similarity between the chemical shifts of the parent piperidine and that of the corresponding 1,1'-bipiperidine.

The assignment of the signals in the high temperature spectra makes possible the grouping of corresponding resonances at the low temperature. Assignment of signals for 7 in the low temperature (at  $-117^\circ\text{C}$ ) spectrum rests on comparison of the experimental chemical shifts with calculated ones (Table 4.2), which were obtained by the following procedure: (i) Chemical shifts for the corresponding hydrocarbon 14 in an appropriate conformation were calculated using the parameters of Dalling and Grant, which were derived from perhydroanthracenes and perhydrophenanthrenes<sup>37)</sup>, since the  $^{13}\text{C}$  chemical shift data of 14 were not available in the literature. (ii) The effects caused by the replacement of two C-H groups by nitrogen atoms were added to the calculated chemical shifts for 14. We assume that the chemical shift change caused by the replacement of the CH groups by nitrogen atoms in 14 is equal to that caused by the replacement of the  $\text{CH}_2$  group by NH in cyclohexane; thus, the chemical shift change of carbon atoms  $\alpha$ ,  $\beta$ , and  $\gamma$  to the replacement center is 21.4, 1.2,

and -0.6 ppm, respectively.<sup>17)</sup>

The following example illustrates the procedure for the signal of C2 in conformation G-SReeee. In the analogous conformation of 14 the tertiary C2 carbon (T) has three carbons in  $\alpha$  and also three carbons in  $\beta$  position; C2 is involved in three Vg interactions (C3-C2-C1-C6, 2Me-C2-C1-C1', C4-C3-C2-C1) and in two Vt interactions (C3-C2-C1-C1', 2Me-C2-C1-C6); the proton attached to C2 is interacting with one of the C6' protons ( $\gamma_{HH}$ ). Hence the predicted chemical shift of the hydrocarbon  $\delta_{BC}(C2)$  is given by

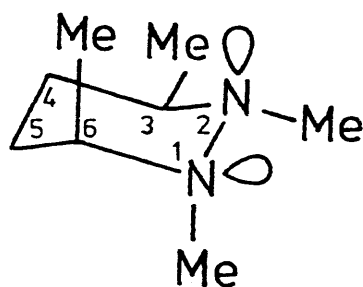
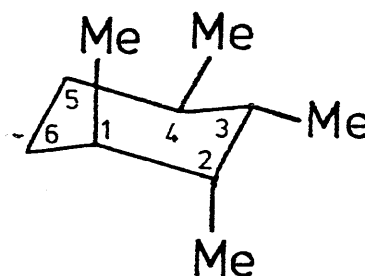
$$\delta_{BC}(C2) = -2.49 + 3\alpha + 3\beta + T + 3V_g + 2V_t + \gamma_{HH} = 33.84 \text{ ppm}$$

By adding the effect of the CH - N replacement we obtain the chemical shift of C2 of 7  $\delta_{BP}(C2)$ :

$$\delta_{BP}(C2) = 33.84 + 21.4 + 1.2 = 56.44 \text{ ppm}$$

In a similar fashion, all of the signals for the ring carbons of G-SReeee and G+SSeeea were calculated. In this calculation it is assumed that the effect of a lone pair is equal to that of a C-H bond in  $\gamma$ -gauche steric interactions. Although this seems to be a poor assumption, the magnitude of the interaction between  $\gamma$ -gauche hydrogens ( $\gamma_{HH}$ ), which is one of the significant steric interactions, has been

proved to be nearly equal to that of the  $\gamma$ -gauche hydrogen and a lone pair interaction by the examination of the literature data;<sup>10)</sup> the chemical shift difference between the 6-axial-CH<sub>3</sub> of 1,2,3,6-tetramethylperhydropyridazine in the conformation 21 ( $\delta$  18.74) and that for 1-axial-CH<sub>3</sub> of 1,2,3,4-tetramethylcyclohexane in the analogous conformation 22 ( $\delta$  18.82), which was calculated from the parameters of Dalling and Grant, is negligibly small (0.08).<sup>38)</sup> On the basis of the comparison of the calculated with the observed chemical shifts, assignment of the signals for C2, C2', C6, and C6' was reliably performed but the differentiation between the signals for C3 and C3', or C4 and C4', or C5 and C5' was unsuccessful since the calculation gives equal values for each sets. The assignment of 2-CH<sub>3</sub> and 2'-CH<sub>3</sub> was made considering the  $\gamma$ -gauche steric interaction.

2122



Assignment of the signals in the low temperature spectra of 8 was performed in a similar fashion except in the case of the peaks for C2 and C6, in which the two peaks were so close that they were not differentiated by the inspection of the signal splitting process in the course of temperature variation but clearly differentiated by the measurement of  $T_1$ ;  $T_1$  of C2', C2, C6, and C6' were 2.0, 1.8, 1.2, and 1.2 s, respectively. Assignment of the four peaks for methyl groups in the low temperature spectrum was made on the basis of the temperature dependence of chemical shifts. Considering steric effects, the larger splitting set was assigned to 2, 2'-CH<sub>3</sub> and the smaller splitting set was assigned to 4, 4'-CH<sub>3</sub>. Thus, assignment of the methyl peaks in the high temperature spectrum was also accomplished.

In the case of 9, assignment of the peaks for C2 and C6 in the low temperature spectrum was similarly made on the basis of the  $T_1$  measurements.

#### 4.8 Molecular Mechanics Calculations

Molecular mechanics calculations were carried out using Allinger's MMI program,<sup>23)</sup> which was partially modified by Osawa, Kureha group, and us without changing the parameters for the force field, on the HITAC M280H computer system of

Computer Centre University of Tokyo. In the calculation of each of the gauche conformations in 14, 15, and 16 (Table 4.4), the full relaxation technique was used, and all structures were optimized without symmetry constraints. The steric energies of the trans conformations (Table 4.4) and the energy profiles for the rotation about the C1-C1' bond of 14, 15, 16, and 17 were calculated using the Wiberg-Boyd bond drive technique.<sup>39)</sup>

## 4.9 References and Notes

- 1) Ogawa,K.; Takeuchi,Y.; Suzuki,H.; Nomura,Y., Chem.Lett., 1981, 697. Idem., J.Chem.Sco., Chem.Comm., 1981, 1015. Idem., J.Am.Chem.Soc., in press.
- 2) An excellent review of the conformational analysis of hydrazines: Shvo,Y., "The Chemistry of Hydrazo, Azo, and Azoxy Groups", Patai,S., Ed.; Interscience: New York, 1975; Part 2, p.1017.
- 3) Rademacher,P.; Koopman,H., Chem.Ber., 1975, 108, 1557. Nelsen, S.F.; Hollised,W.C., J.Org.Chem., 1980, 45, 3609.
- 4) Tanaka, M; Takeo, H; Matsumura, C; Yamanouchi, K; Kuchitsu, K; Fukuyama, T., Chem.Phys.Lett., 1981, 83, 246.
- 5) The synthesis of the acyclic hydrazines with the torsion angle of ca.  $180^\circ$ , in which large steric crowding about the N-N bond exists, has been reported. Nelsen, S.F.; Hollinsed, W.C.; Kessel, C.R.; Calabrese, J.C., J.Am.Chem.Soc., 1978, 100, 7876. Nelsen, S.F; Gannett, P.M., Ibid., 1982, 104, 5259.
- 6) Lister,D.C; Macdonald,J.N; Owen,N.L., "Internal Rotation and Inversion"; Academic Press: London, 1978. Chapter 7.
- 7) Jones,R.A.Y.; Katritzky,A.R.; Scattergood,R., J.Chem.Soc., Chem.Comm., 1971, 644. Jones,R.A.Y.;

- Katritzky, A.R.; Record, K.A.F.; Scattergood, R.,  
J.Chem.Soc., Perkin Trans.2, 1974, 406.
- 8) Anderson, J.E., J.Am.Chem.Soc., 1969, 91, 6374.
- 9) Anderson, J.E.; Griffith, D.L.; Roberts, J.D.,  
J.Am.Chem.Soc., 1969, 91, 637. Dewar, M.J.S.;  
Jennings, W.B., J.Am.Chem.Soc., 1973, 95, 1562.
- 10) Nelsen, S.F.; Weisman, G.R., J.Am.Chem.Soc., 1976, 98,  
3281. Weisman, G.R.; Nelsen, S.F., Ibid., 1976, 98, 7007.  
Nelsen, S.F., Acc.Chem.Res., 1978, 11, 14.
- 11) Shvo designated a single-passing rotation and a double-  
passing rotation as a low energy rotation and a high  
energy rotation, respectively (See ref. 2).
- 12) Lattimer, R.P.; Harmony, M.D., J.Am.Chem.Soc., 1972, 94,  
351.
- 13) Literature through 1973 was cited in ref. 2).  
Riddell, F.G., "The Conformational Analysis of  
Heterocyclic Compounds"; Academic Press: London, 1980;  
Chapter 2. Jarvie, J.O.; Rauk, A., Can.J.Chem., 1974,  
52, 2785. Jarvie, J.O.; Rauk, A.; Edmiston, C.K.,  
Ibid., 1974, 52, 2778. Viktovskaya, N.M.; Dolgunicheva,  
O.Yu.; Frolov, Yu.L.; Keiko, V.V.; Voronkov, M.G.,  
Dokl.Akad.Nauk SSSR, 1977, 235, 843. Brunk, T.K.;  
Weinhold, F., J.Am.Chem.Soc., 1979, 101, 1700. Cowley,  
A.H.; Mitchell, D.J.; Whangbo, M-H.; Wolfe, S., Ibid.,  
1979, 101, 5224. Chiu, N.S.; Sellers, H.L.; Schafer, L.;

- Kohata,K., Ibid., 1979, 101, 5883. Imamura, A.; Ohsaku, M., Tetrahedron, 1981, 37, 2191.
- 14) Fletcher,J.R.; Sutherland,I.O., J.Chem.Soc., Chem.Comm., 1969, 706.
- 15) Nomura,Y.; Ogawa,K.; Takeuchi,Y.; Tomoda,S., Chem.Lett., 1978, 271. Ogawa,K.; Nomura,Y.; Takeuchi,Y.; Tomoda,S., J.Chem.Soc., Perkin Trans 1, 1982, 3031.
- 16) Eliel,E.L.; Kandasamy,D.; Yen,C.; Hargrave,K.D., J.Am.Chem.Soc., 1980, 102, 3698.
- 17) Booth,H.; Griffiths,D.V., J.Chem.Soc., Perkin Trans.2, 1973, 842.
- 18) Roberts,J.D.; Weigert,F.J.; Kroschwotz,J.I.; Reich,H.J., J.Am.Chem.Soc., 1970, 92, 1338.
- 19) Burke,J.J.; Lauterbur,P.C., J.Am.Chem.Soc., 1964, 86, 1870.
- 20) Vold,R.L.; Waugh,J.S.; Klein,M.P.; Phelps,D.E., J.Chem.Phys., 1968, 48, 3831. Freeman,R.; Hill,H.D.W., Ibid., 1969, 51, 3140.
- 21) Binsch,G., "Topics in Stereochemistry"; Allinger,N.L.; Eliel,E.L. Ed.; Wiley Interscience: New York, 1968; Vol.3, p.97. Abraham,R.J.; Loftus,P., "Proton and Carbon-13 NMR Spectroscopy"; Heyden & Son: London, 1978; Chapter 7.
- 22) Anet,F.A.L.; Anet,R., "Dynamic Nuclear Magnetic Resonance Spectroscopy"; Jackman,L.M.; Cotton,F.A., Ed.;

- Academic Press: New York, 1975; Chapter 14.
- Lambert, J.B.; Featherman, S.I., Chem.Rev. 1975, 75, 611.
- Katritzky, A.R.; Patel, R.C.; Riddell, F.G., Angew.Chem., Int.Ed.Engl., 1981, 20, 521.
- 23) Allinger, N.L., Quantum Chemistry Program Exchange, Indiana University, 1975, Program 318.
- 24) During the course of our work, Prof. E. Ōsawa has obtained similar results using MM2 for cyclohexylpiperidines (personal communication).
- 25) Ōsawa, E.; Shirahama, H.; Matsumoto, T., J.Am.Chem.Soc., 1979, 101, 4824. Beckhause, H-D.; Ruchardt, C.; Anderson, J.E., Tetrahedron 1982, 38, 2299. Ōsawa, E.; Musso, H., "Topics in Stereochemistry"; Allinger, N.L.; Eliel, E.L. Ed.; Wiley Interscience: New York, 1982; Vol.13, p 117 and references therein.
- 26) Theilacker, W.; Bohm, H., Angew.Chem., Int.Ed.Engl., 1967, 6, 251.
- 27) Wendisch, D.; Feltkamp, H.; Sheidegger, U., Org.Magn.Reson., 1973, 5, 129.
- 28) Ladenburg, A., Justus Liebigs Ann.Chem., 1888, 247, 1.
- 29) Booth, H.; Little, J.H., J.Chem.Soc., Perkin Trans.2, 1972, 1846.
- 30) Feltkamp, H.; Naegele, W.; Wendisch, D., Org.Magn.Reson., 1969, 1, 11.
- 31) Ziegler, K.; Zeiser, H., Chem.Ber., 1930, 63, 1847.

- Bohlmann,F.; Englisch,A.; Politt,J.; Sander,H.;  
Weise,W., Chem.Ber., 1955, 88, 1831.
- 32) Schöllkopf,U.; Paust,J.; Patsch,M.R., Org.Syntheses,  
Coll.Vol. 5, 1973, 859.
- 33) Prepared by Professor S.Nishimura.
- 34) Kleier,D.A.; Binsch,G., Quantum Chemistry Program  
Exchange, Indiana University, 1970, Program 165.
- 35) Binsch,G.; Kessler,H., Angew.Chem., Int.Ed.Engl., 1980,  
19, 411.
- 36) Bevington,P.R., "Data Reduction and Error Analysis for  
the Physical Science"; McGraw-Hill: New York, 1969;  
Chapter 4.
- 37) Dalling,D.K.; Grant,D.M., J.Am.Chem.Soc., 1974, 96,  
1827.
- 38) Dalling,D.K.; Grant,D.M., J.Am.Chem.Soc., 1972, 94,  
5318.
- 39) Wiberg,K.B.; Boyd,R.H., J.Am.Chem.Soc., 1972, 94, 8426.